

Cenozoic Faults and Seismicity in Northwest Saudi Arabia and the Gulf of Aqaba Region

M. John Roobol and Ian C. F. Stewart

Abstract

Following the November 1995 earthquake in the Gulf of Aqaba that affected countries in the area including northwest Saudi Arabia, a study was made to identify the youngest geological faults in the area. These faults have been termed Cenozoic faults, although most are Neogene in age, being younger than 23 Ma. A number of previously unknown structures have been identified. These include a zone of shattered and intensely faulted rocks 25 km wide that extends inland into Saudi Arabia from the coast of the Gulf of Aqaba. In this zone, shattered granite intrusions are eroded in a similar manner to sandstone and produce deep, vertical walled, narrow gorges, such as Tayyib al Ism. Faults parallel to the Gulf of Aqaba occur as deep wadis where the geological contacts are offset by sinistral displacements of up to 9 km, and show systematic shoulder uplift away from the gulf. Another major Cenozoic structure contained within the Saudi Arabian side of the Gulf of Aqaba is a major fold that extends 50 km inland from the coast. In this fold the Precambrian lithologic units, dikes and faults are rotated 90 degrees anticlockwise with the appearance of a drag fold due to the approximately 115 km sinistral offset of the Gulf of Aqaba. This structure is not repeated in Sinai and occurs only on the Arabian side of the Gulf. It is interpreted not as a drag fold but as a fold that probably resulted from the initial displacement along the Arabian Plate from Sinai. Later faults isolated the structure within Saudi Arabia. Reactivated Precambrian faults within the structure are also curved. Aeromagnetic anomalies show that the traces of major Tertiary gabbro dikes that parallel

the Red Sea coast of Saudi Arabia are also curved within the fold, but their curvature of about 45 degrees anticlockwise is less than that of the Precambrian rocks and dikes, which suggests dike emplacement occurred after folding commenced. Maps that cover an area 550 km east-west by 360 km north-south and include the Gulf of Aqaba and adjacent areas show the whole area to be cut by thousands of Cenozoic faults (about two and a half thousand of the larger faults are shown here). The oldest faults occur in a 250-km wide belt of pre-rift structures that include graben structures that lie to the east of the Gulf of Aqaba fault system. These faults are oriented north-northwest in the north and curve to the northwest in the south of the study area, and are named Ribbon faults because they divide the country rocks into long thin strips from 100 to 500 m wide. These faults mainly occur within Paleozoic sandstone where they are preserved as walls cemented by iron oxides/hydroxides. Where the Ribbon faults occur within Precambrian Shield and Tertiary sediments the oxide/hydroxide fills are absent. The Ribbon faults result from crustal extension as they form horst-graben structures with topography of a few metres. In some areas open fissures occur without apparent displacement. The aeromagnetic maps show that some of the major graben structures are underlain by large Tertiary gabbro dikes. The system is mainly seismically inactive today with a few local exceptions, such as a cluster of earthquake activity about 75 km southeast of Tabuk city. Most active are the north-south to north-northeast-trending Gulf of Aqaba system of faults that include those of the floor of the Gulf of Aqaba. Other notable fault systems in the area are a prominent set of pre-rift east-west faults, some of which contain traces of Tertiary gabbro dikes and some of which become curved toward the Gulf of Aqaba like the reactivated Precambrian faults. The map area preserves a record of about 25 million years of faulting that commenced in pre-Red Sea rift time, and also records the initiation of separation of the Arabian Plate from Sinai by fold deformation prior to

M. J. Roobol (✉)

The Anchorage, Sandy Haven, St. Ishmaels, Haverfordwest,
Pembrokeshire, SA62 3DN, UK
e-mail: roobolinc2000@hotmail.com

I. C. F. Stewart

Stewart Geophysical Consultants Pty. Ltd, Adelaide, SA 5069,
Australia
e-mail: stewgeop@senet.com.au

faulting. Some minor folding occurs from drag and compression of a belt of Tertiary sedimentary rocks originally continuous with the Gulf of Suez which were transported 115 km into the Gulf of Aqaba. The Gulf of Aqaba region remains the most active seismic area in Saudi Arabia and is the site of three large earthquakes in 1983, 1993 and 1995.

1 Introduction

Several of the most powerful earthquakes experienced in Saudi Arabia during recent decades were centred in the Gulf of Aqaba and affected the inhabited areas of northwest Saudi Arabia, especially the town of Haql (Figs. 1 and 2). These include the 1983 swarm, with a maximum magnitude M_I of 5 (El Isa et al. 1984), a swarm in 1993 with a maximum M_w of 6.1, and the November 1995 M_w 7.3 event (Smith and Bokhari 1984; Bazzari et al. 1990; Klinger et al. 1999; Roobol et al. 1999). Following the latter magnitude 7.3 event a geological investigation was initiated by the Saudi Geological Survey to identify the youngest fault systems responsible for these earthquakes. The results of this study for the northwest of Saudi Arabia and adjacent regions are presented here in a revised version of that given by Roobol and Stewart (2009), including more recent seismicity data.

The study area forms the westernmost part of the Arabian lithospheric plate at the junctions of the Red Sea and Gulf of Aqaba. Today, the Red Sea is a young ocean basin with a central spreading axis opening at a mean rate of about 16 mm per year, with a present-day rate of 24 ± 1 mm/year in the south (at 12°N) and 7 ± 1 mm/year in the north (Reilinger et al. 2015). The opening of the Red Sea is considered to have taken place in two stages that correspond to two distinct volcanic episodes along the western margin of the Arabian Plate (Camp and Roobol 1992). An earlier stage of rifting occurred between about 30 to 20 Ma, followed by a later stage of rifting during at least the past 5 million years and possibly 10 million years (Girdler and Southren 1987; Bayer et al. 1988; McGuire and Bohannon 1989; Bohannon et al. 1989; Johnson 1998). The deeply-eroded fault boundary between the Cenozoic coast plain sediments and the Precambrian shield has been named the “Master Listric Coastal Fault” by Roobol and Kadi (2008).

The Stage 1 opening of the Red Sea corresponded to the eruption of the older Tertiary harrats (lava fields) of western Saudi Arabia between about 30 and 14 Ma. The second stage of opening resulted in the formation of the 200-km long Gulf of Aqaba and its 1,000 km extension as the Dead Sea Rift Zone. This is a left lateral transform fault system that forms the northwest boundary of the Arabian Plate. It is

essentially a number of subparallel sinistral transform faults with associated pull-apart basins. The Stage 2 opening corresponds to the formation of the younger harrats of the western Arabian Plate from about 10 Ma to the present time. Ben-Avraham et al. (2008) estimate the sinistral motion on the Gulf of Aqaba and Dead Sea Rift to be approximately 5–7 mm/year. Reilinger et al. (2015) suggest that at the southern end of the Gulf of Aqaba the left-lateral motion of Arabia with respect to Sinai is 4.5 mm/year with 2.2 mm/year extension. From GPS measurements, the present slip rate on the Wadi Araba Fault section of the Rift immediately to the north of the Gulf of Aqaba is given by al Tarazi et al. (2011) as 4.9 ± 0.4 mm/year, while Sadeh et al. (2012) obtained a slip rate of 4.7–5.4 mm/year. Reilinger et al. (2015) indicate that there is almost pure left lateral strike slip with a geodetic slip rate along the southern Dead Sea Fault of 4.4 ± 0.3 mm/year where they quote a total post-Late Miocene (11 Ma) offset on the Fault of 45 ± 5 km. The fault zone is described as a transform and not a transcurrent fault because it separates two tectonic plates. Ben-Avraham (1985) describes it as “a plate boundary of the transform type that connects the Red Sea, where seafloor spreading occurs, with the Zagros-Taurus zone of continental collision”. He also notes that it “is of particular interest because it is one of the two places in the world (the Gulf of California-Imperial Valley is the other), where a mid-ocean ridge system changes into a transform system and runs into a continent”.

The fault-bounded Maqna Block of Tertiary sedimentary units measures 50 km by 50 km (Fig. 3) and constitutes the extreme western point of Saudi Arabia. Internally the sedimentary units are folded into an anticlinorium in the west (with a core of Precambrian rocks) and a synclinorium in the east. Following Stage 1 opening of the Red Sea–Gulf of Suez, this large block of Tertiary sediments was part of the Tertiary sedimentary belts that line the margins of the Gulf of Suez and the early Red Sea (Coleman 1977). The Maqna Block can be regarded as part of the Gulf of Suez Tertiary sedimentary belt that has been displaced 115 km into the present Gulf of Aqaba by sinistral movement along the Aqaba-Levant fault system. The folding of the Tertiary sediments into an anticlinorium with a core of Precambrian basement and associated synclinorium is believed to result from lateral compression of the Maqna Block as it was transported into the Aqaba-Levant fault system.

A first attempt to fit the data shown here to a Landsat base failed because detailed structures could not be seen or positioned accurately. However, when the Shuttle Radar Topography Mission (SRTM) topographic grid data became available in 2000, it was found to be ideally suited to the deserts of Saudi Arabia, where the lack of vegetation enables the detailed SRTM information to be a good approximation

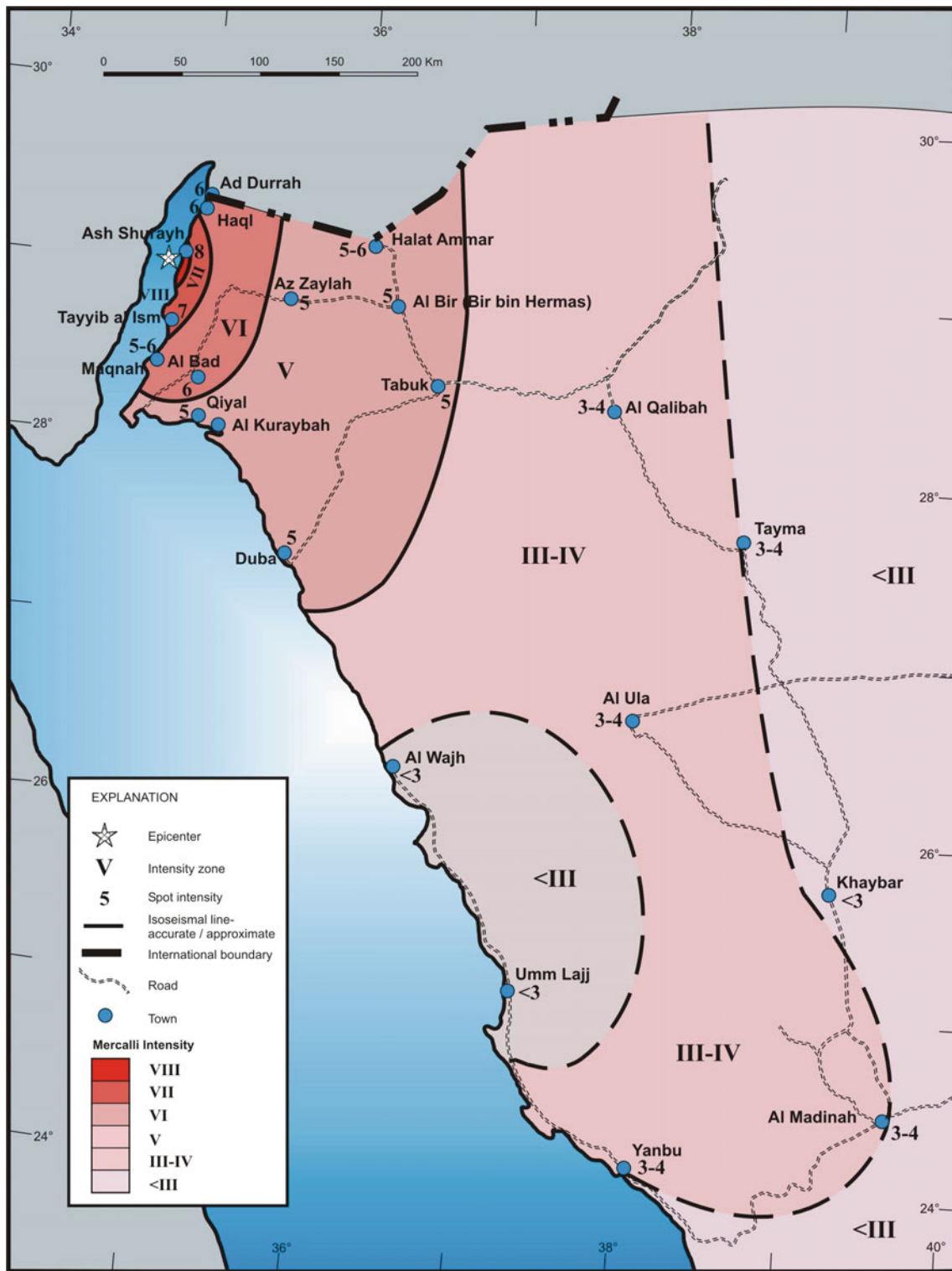


Fig. 1 Isoseismal map of the effects of the Gulf of Aqaba earthquake of November 22, 1995 in Saudi Arabia, showing zones of Mercalli intensity (after Roobol et al. 1999)



Fig. 2 One of the fault scarps of November 22, 1995 in the zone of epicentral rupture. The scarp is 40 cm high and the fault shows 10 cm of opening. It is situated at the foot of a prehistoric fault scarp 12 m high in unconsolidated Quaternary/Tertiary fanglomerate. The location is latitude 29°02'44.97" N, longitude 34°51'36.84" E

to the actual surface elevation. A 200-m grid of the SRTM data on a UTM projection is shown in Fig. 4, where the colour interval is 100 m and the maximum height is 2608 m above sea level. The first vertical derivative (FVD) for the northern half of this area is shown in Fig. 5 in order to accentuate local variations used here for the analysis of structural trends and faults. In this FVD image locally high values are white or light and low values are dark.

Many of the main structural trends can also be observed on images of aeromagnetic data, which were only available to us for that part of the study area within Saudi Arabia. The magnetic grid used here was compiled from a number of airborne surveys carried out over the Precambrian shield and adjacent Phanerozoic rocks, as described by Zahran et al. (2003). The reduced-to-the-pole (RTP) magnetic grid is shown in Fig. 6, where high values are red and low values are blue or purple.

2 Structure of the Gulf of Aqaba

The 200-km long Gulf of Aqaba with its 1,000-km extension as the Aqaba-Levant fault system, which includes the Dead Sea Rift Zone, has a long history of seismic activity (Al-Amri et al. 1991; Ben-Avraham et al. 1979, 2008; Hamiel et al. 2009). A paleoseismic study of the Lebanese section by Daëron et al. (2007) indicated that there have been 10–12 major earthquakes in the past 12,000 years. A similar study of the Jordanian section by Klinger et al. (2015) indicated 9 major earthquakes in the past 5,000 years. The November 1995 earthquake had a moment magnitude M_w of 7.3 with an epicentre just off the Saudi Arabian coastline. A 20-km long section of uninhabited coastline south of Haql showed epicentral rupture (Fig. 2; Williams et al. 2001), and aftershocks continued into 1996. Modelling of InSAR data by Klinger et al. (2000a) indicates that this event was due to mainly left-lateral slip of 2.1 m along a 56 km-long fault striking N195°E between the Elat (Eilat) and Aragonese Deep.

The structure of the Gulf of Aqaba has been described by Ben-Avraham et al. (1979) and Ben-Avraham (1985) and the fault data is included in Fig. 7 (based on the FVD of the SRTM topography image in Fig. 5), which also includes data taken from Bender (1975) and Eyal et al. (1980). The major faults visible on the SRTM base maps are included in Fig. 7, but there are many smaller ones that are not shown here. In its simplest form, the Gulf of Aqaba can be regarded as a series of sinistral transform fault controlled pull-apart basins or rhomb-shaped grabens that are in places more than 10 km deep (Ben-Avraham et al. 2008). However, as pointed out by Ben-Avraham (1985) this is oversimplified and the structures are more complex. The steep sea cliffs along the northeastern shore of the Gulf of Aqaba are fault zones of shattered rock that plunge into the deep waters of the pull-apart basins of the Gulf (Fig. 8). There is an anti-clockwise rotation of the Arabian Plate of 0.37° per Myr relative to Nubia (Reilinger et al. 2006; ArRajehi et al. 2010), as indicated by the width of the Red Sea between the shoulders of Precambrian basement. These are about 200 km apart in the north at latitude 27 degrees north and 350 km apart in the south at latitude 17 degrees north. The rotation requires a progressive opening of the Gulf of Aqaba so the basins become wider with time.

3 Asymmetric Shoulder Uplift Along the Red Sea

The Precambrian shield on both sides of the Red Sea, like that on either side of the Gulfs of Suez and Aqaba, shows topographic shoulders. The phenomenon is clearly expressed

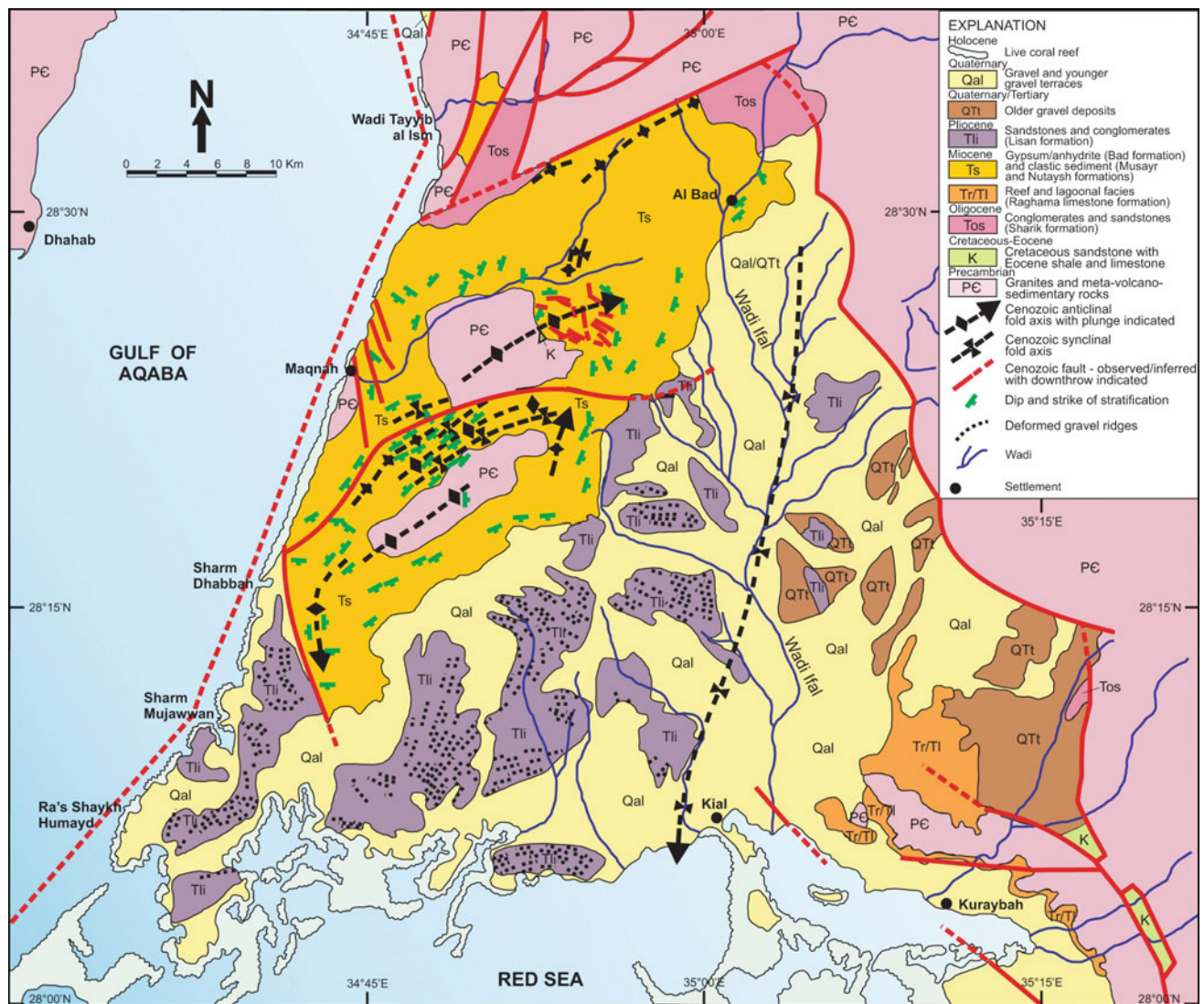


Fig. 3 Cenozoic folding and sedimentary units in the Maqna Block (modified after Motti et al. 1982; Bayer et al. 1988)

in Saudi Arabia along the road leading from the Red Sea port of Duba to the inland city of Tabuk. The road crosses the Red Sea coastal plain and then climbs the Red Sea escarpment to come out on the exhumed peneplain on top of the Precambrian shield that is overlain by erosional outliers of Cambrian/Ordovician Saq Sandstone. Looking northwest toward the Gulf of Aqaba, the exhumed peneplain with its cap of reddish sandstone can be seen to rise systematically toward the Gulf. Along the Saudi Arabian side of the Gulf of Aqaba considerable shoulder uplift has occurred of the Precambrian rocks which rise to a maximum of 2,580 m on Jabal Laws. Similarly, along the length of the Red Sea there are distinctive shoulders along the escarpments, as shown in Fig. 4. Fission track ages of apatite (Bohannon et al. 1989) have dated the uplift to between 13.8 and 5 Ma, and these

dates suggest that 2.5–4 km of uplift occurred along the Arabian escarpment during the past 13.8 million years.

The escarpment crest on the eastern side of the Red Sea is higher than that on the west. The presence of topographic shoulders, but not the asymmetry, was regarded as due to isostatic rebound, possibly because of erosion of the cover. A mechanism proposed by Doglioni et al. (2003) that accounts for the asymmetry as a worldwide phenomenon associated with ocean ridges and rifts requires that depleted and lighter asthenosphere generated below an ocean ridge is shifted eastward relative to the lithosphere, resulting in a density deficit below the eastern flank so that the lithosphere rises or is buoyed up. Their model suggests that the westward drift of the lithosphere relative to the underlying mantle might be a global phenomenon.

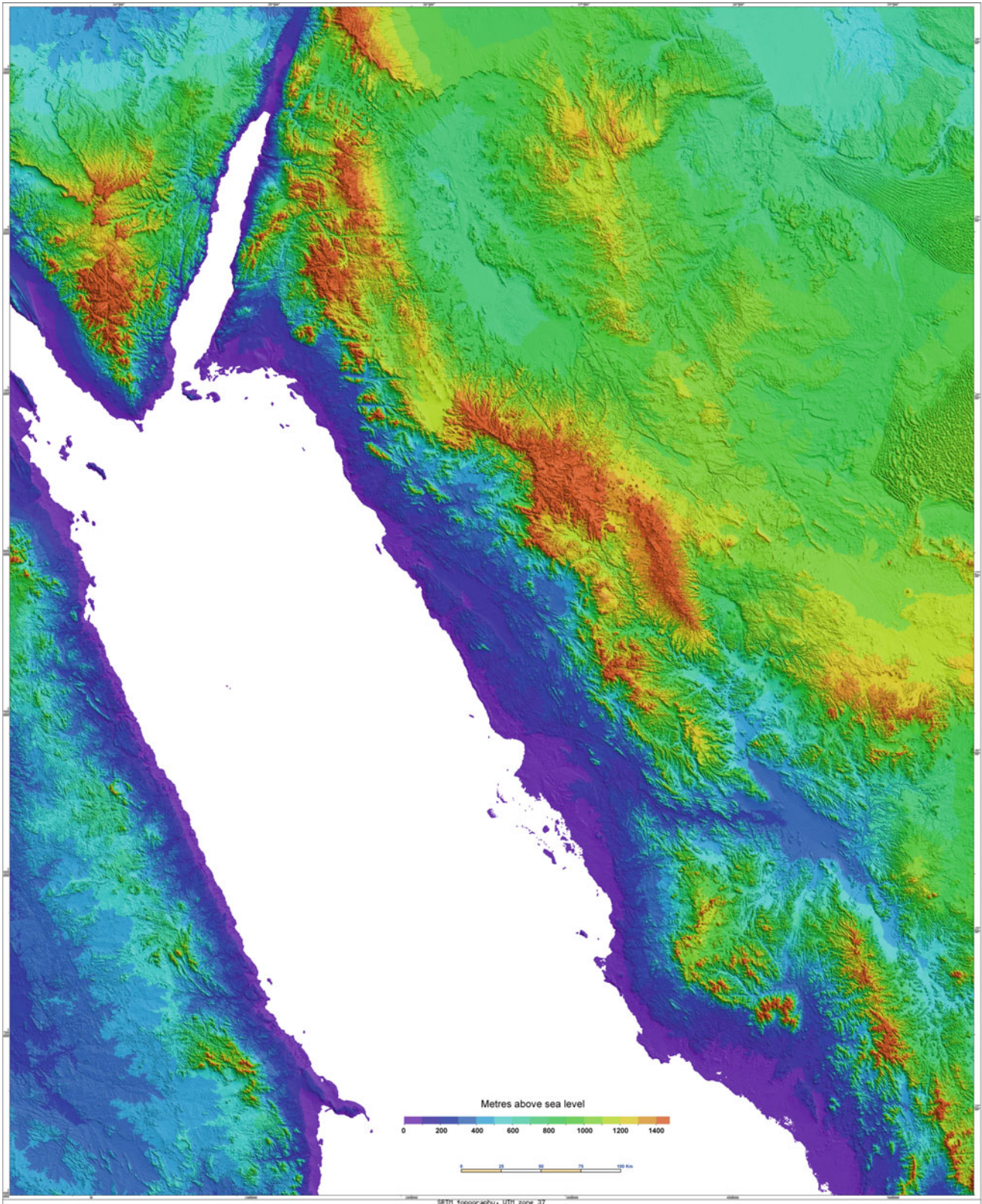


Fig. 4 Shuttle Radar Topography Mission (SRTM) surface elevation, around northern Red Sea and northwest Saudi Arabia, showing uplifted shoulders on both sides of the Red Sea including southern Sinai. The

uplift is higher on the eastern side of the Red Sea. In northwest Saudi Arabia the Cenozoic lava field of Harrats Ar Raha and Uwayrid lies on top of the Red Sea coastal escarpment

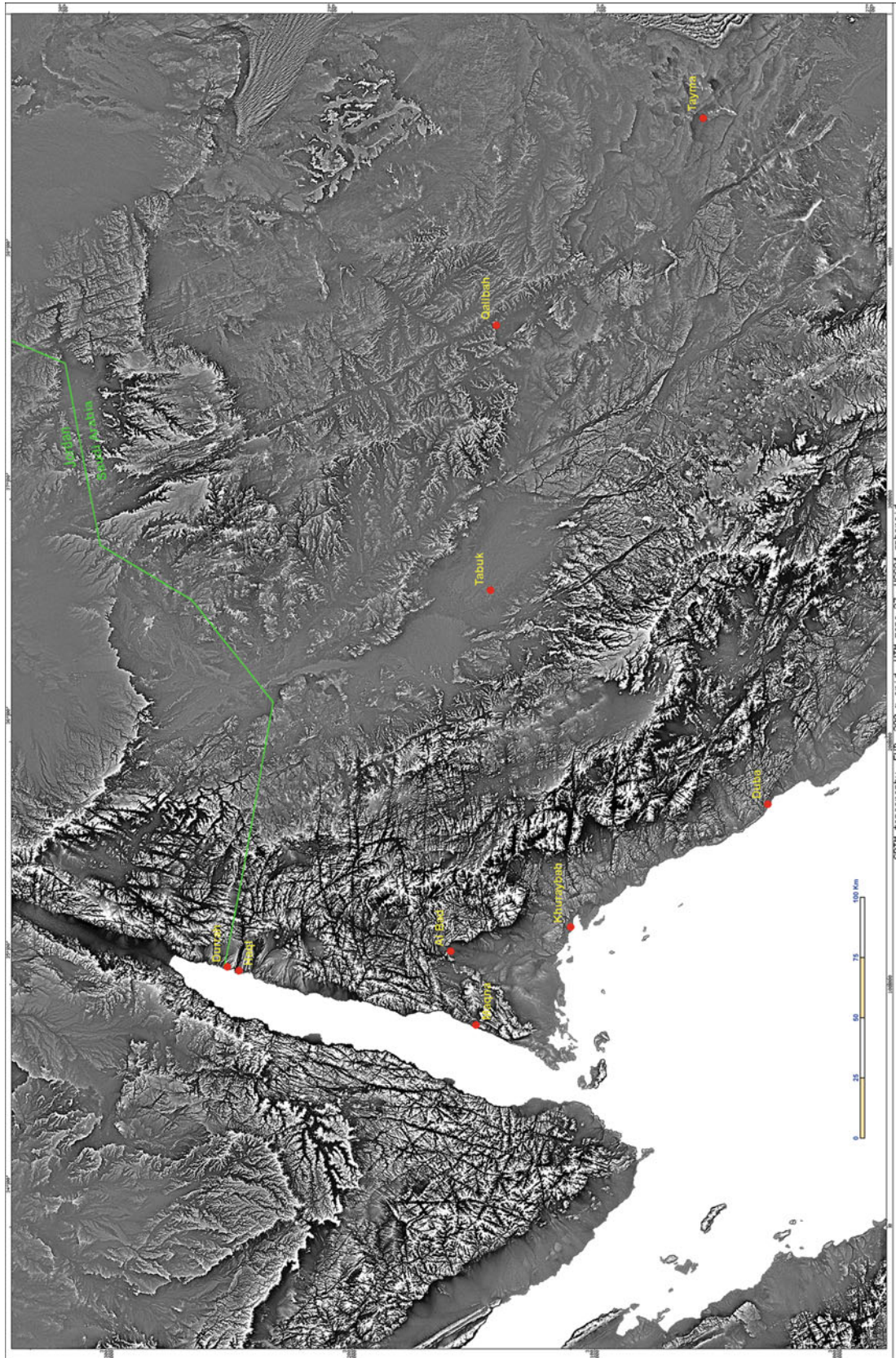


Fig. 5 SRTM surface elevation, first vertical derivative, northwest Saudi Arabia and adjacent areas

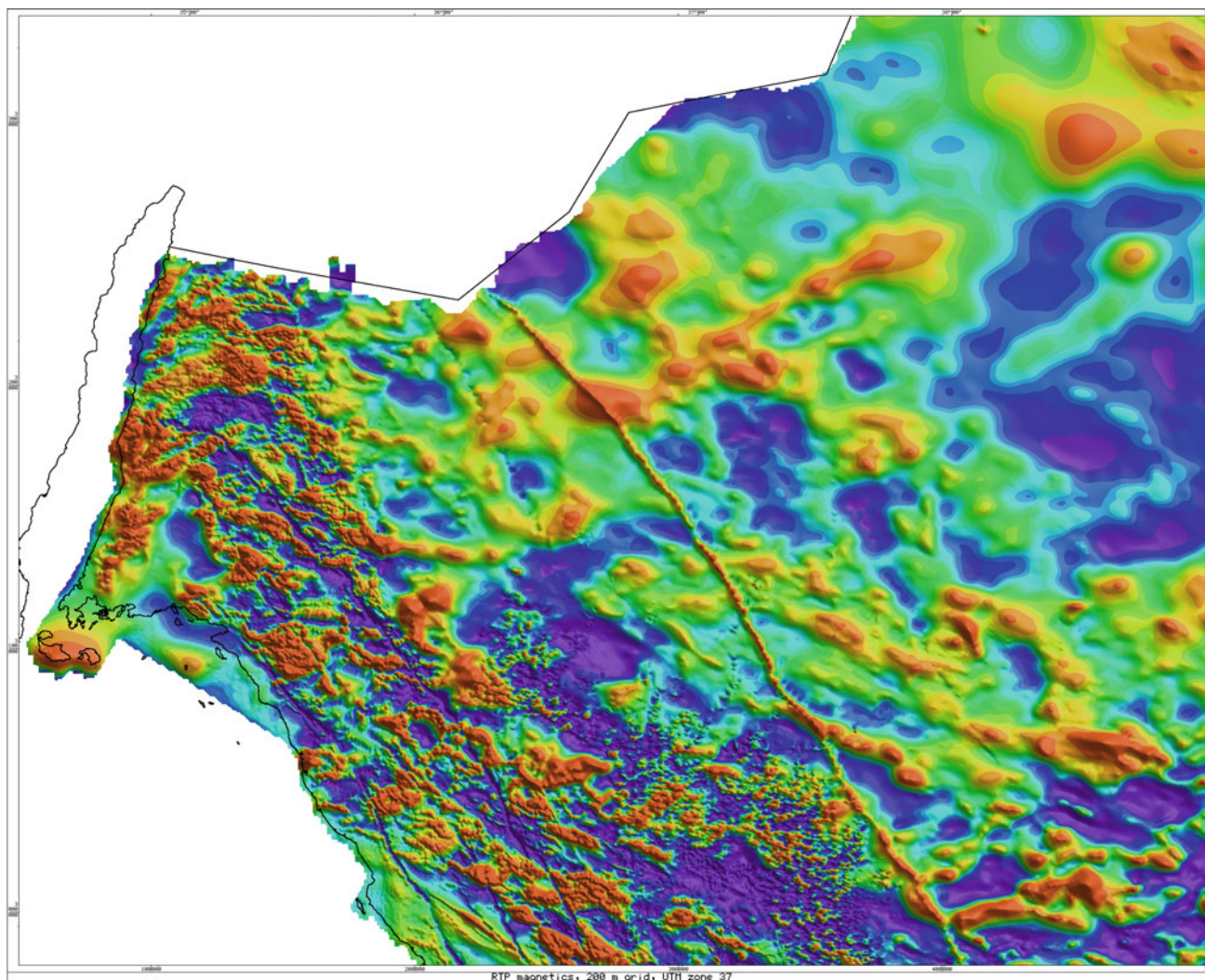


Fig. 6 Reduced to the pole aeromagnetic map of northwest Saudi Arabia

4 Recognition of Cenozoic Faults

In the course of this work a number of criteria evolved to separate Cenozoic from Precambrian faults. Cenozoic faults were readily identified because they offset the coastal Tertiary sediment such as the yellow-weathering green siltstone and sandstone. Another valuable tool was the Quaternary raised reefs, composed of resistant reef-facies limestone and more friable lagoonal facies calcarenites. Along the margins of the Red Sea, the Lower Miocene Raghama limestone provided a good reference rock that is cut by Cenozoic faults. The Raghama paleoreef is remarkably well preserved along the northernmost 600 km of Red Sea coastline where it coats the deeply-eroded Master Listric Fault that separates the coast plain Cenozoic sediments from the Precambrian shield. The internal structure of the limestone is exposed in

gorges eroded through it, and commonly the limestone shows steep fore-reef bedding in the reef front facies which is often successively overlain by flat bedded limestones that overlap the foreset bedding. The top of the reef is flat and approximates the Lower Miocene sea level. This is also a valuable reference surface to use to identify Cenozoic faults. Along the front of the Raghama limestone reef are patches of black limestone where hot springs deposited Pb-Zn-Ag sulfide minerals now weathered to secondary minerals at the surface. The best known of these localities is the Jabal Dhaylan base-metal prospect (Hayes et al. 2002). Some of these sites were mined by the Nabatean people whose tombs, like those of Petra in Jordan and Madain Saleh in Saudi Arabia are found at Al Bad within the Maqna Block. Many of these ancient mining areas are now fenced off as archaeological sites.

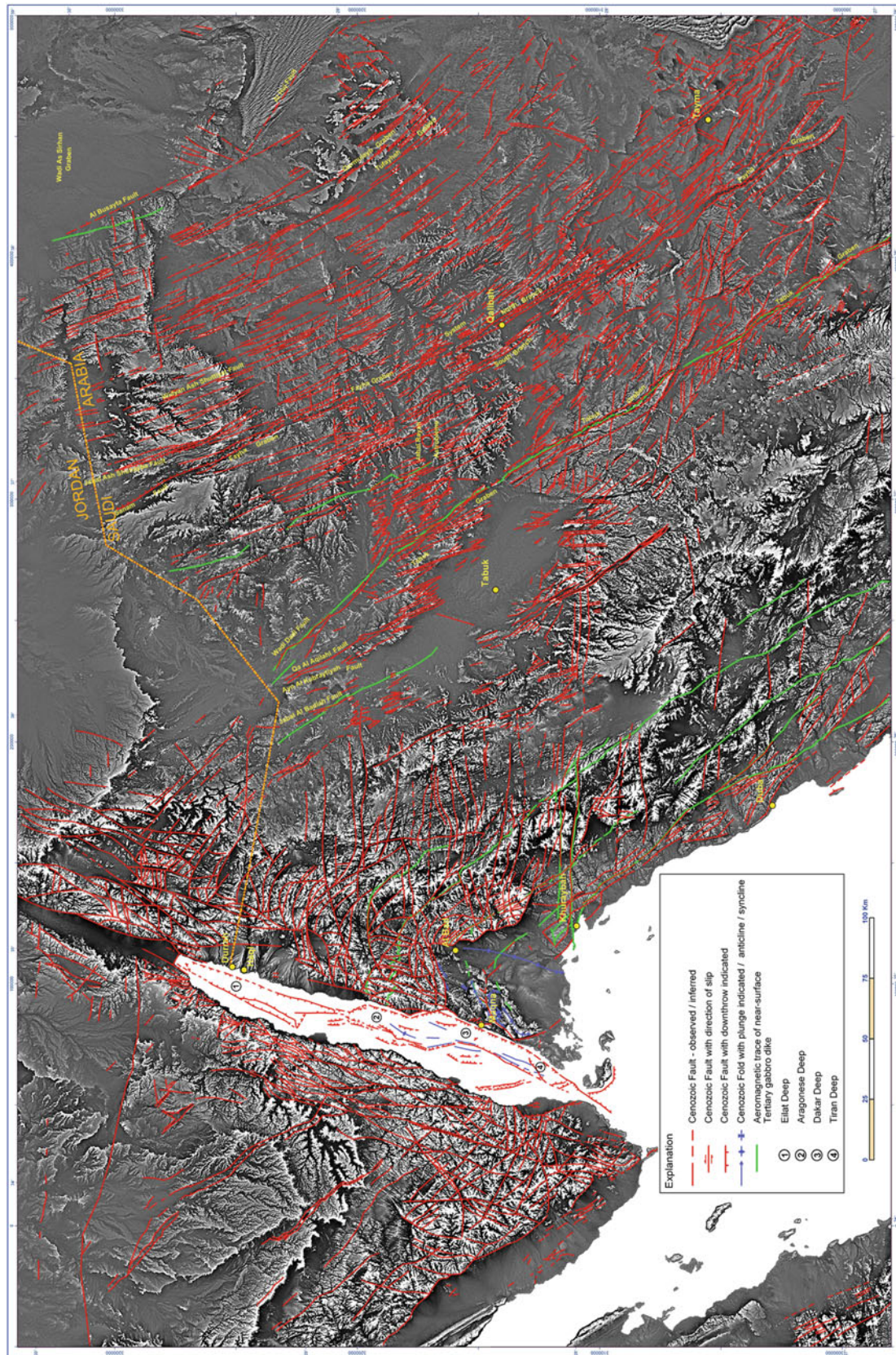


Fig. 7 SRTM surface elevation, first vertical derivative showing Cenozoic faults and folds of northwest Saudi Arabia and adjacent areas. Fault locations in the Gulf of Aqaba from Ben-Avraham (1985)



Fig. 8 Walls of shattered granite oriented parallel to the Gulf of Aqaba. The walls are separated by cataclastic zones of finely crushed rock that erode more rapidly. The coast line here is a fault zone that

plunges to water depths of 1,100 m in the Aragonese Deep. The location is latitude 28°35'34.09"N, longitude 34°47'32.95"E

Another valuable indicator of Cenozoic faulting is found immediately behind or inland of the Raghama Limestone where the flat upper limestone surface continues inland as a broad series of marine terraces cut into the Precambrian shield. Directly north of Duba this marine peneplain is capped by erosional remnants of flat-bedded lagoonal facies Raghama Limestone. The marine peneplain is up to 30 km wide between Kuraybah and Al Wajh and although dissected by erosion can be seen to rise from the flat top of the Raghama (usually around 110 m above sea level (a.s.l.)) in a series of steps to over 300 m a.s.l. and is terminated abruptly in high raised sea cliffs (Fig. 9). Some of the latter are spectacular where they have cut into granite plutons of the Arabian Shield. The marine peneplain provides a datum surface in which uplift of slices of the Precambrian shield bounded by the Red Sea fault systems (sub parallel to the Red Sea coastline) is obvious.

Having recognized horst blocks bounded by Cenozoic faults (relative to the marine peneplain) another criterion of Cenozoic fault recognition emerged. Within areas of Precambrian shield where there may or may not be a preserved marine peneplain, the Cenozoic fault scarps can be

recognized because they produce broad fluvial debris aprons that have been mapped as piedmont fan deposits. The many terrace deposits on the Red Sea coastal plain are all coarse grained and dark in colour with a patina of desert varnish. However, the piedmont fan deposits that radiate away from the Cenozoic fault scarps in fans up to 10 km long are very fine grained and lack desert varnish. These light coloured fans and their adjacent linear fault scarps can be recognised on satellite and Google Earth images.

Since there are many sets of Cenozoic faults as well as Precambrian faults in the area, down-dropped blocks of pre-rift Cretaceous and Tertiary sedimentary rocks occur adjacent to the Red Sea within the Precambrian shield. The largest of these blocks is the Wadi Azlam graben immediately south of the coastal town of Duba on the Red Sea coastal plain at latitude 27°N. The northwest oriented graben is 85 km long in Saudi Arabia and the other half is found in Egypt where it is known as the Quseir Basin (Alabouvette et al. 1979). Other smaller down-dropped blocks within the Precambrian basement occur near the village of Khuraybah and one of these has yielded the first dinosaur bones found in Saudi Arabia (Hughes and Filatoff 1994; Hughes and



Fig. 9 The foreground shows a broad marine platform cut into the Precambrian shield after Stage 1 opening of the Red Sea. The platform exists along the northwest coast of Saudi Arabia from Doha northward.

In the distance are high former sea cliffs cut into late granite intrusions. The location is latitude 27°34'31.76"N, longitude 35°36'04.85"E

Johnson 2005). Two small blocks occur east of the Gulf of Aqaba. One is a small block of Cretaceous-Eocene sediment present on the southern flanks of Jabal Hazma that was described by Motti et al. (1982). The second block is a larger graben of Cambrian/Ordovician Saq Sandstone that has been down-dropped about 2000 m into the basement. The graben is tilted so the Saq Sandstone remains only on the northeast corner and the unconformity overlying the Precambrian surface is exposed (Fig. 10). The block is contained between two E-W faults.

Our interpretation of Cenozoic faults of northwest Saudi Arabia and adjacent areas is shown on a simplified geological map in Fig. 11. The geology is based on maps by Bender (1975), Eyal et al. (1980), and 1:250,000 quadrangle maps for the Kingdom of Saudi Arabia, and data has also been taken from Ben-Avraham et al. (1979) and Ben-Avraham (1985). Inconsistencies in the previous mapping of the Cretaceous and Tertiary across the

Jordan-Saudi Arabia border were resolved using unpublished data from a pterosaur fossil collected recently in the region by Dr. Thomas Rich (pers. comm.). These paleontological data showed that some areas mapped earlier as Tertiary in Saudi Arabia are in fact obviously Cretaceous in age. Faults in the Gulf of Aqaba are compiled from Ben-Avraham (1985).

5 The North-South to North-Northeast-Trending Gulf of Aqaba Fault System

Numerous north-south to north-northeast-trending faults up to 50 km long are parallel and subparallel to both shores of the Gulf of Aqaba (Fig. 7). These faults are best developed on the Sinai side in a belt up to 40 km wide, and are less common but still conspicuous on the Arabian side of the



Fig. 10 Down-dropped Saq sandstone in Precambrian basement. This graben is exposed on both sides of the asphalt road between Haql and Al Bad. The location is latitude 29°02'22.25"N, longitude 35°10'41.69"E

Gulf. The faults all show sinistral displacement that can be measured by the horizontal offset of distinctive rock units (Precambrian markers) as described by Eyal et al. (1981), who record sinistral displacements totalling 18–20 km on both sides of the Gulf of Aqaba. The amount of sinistral displacement on the faults increases toward the Gulf of Aqaba. The three largest of these faults in Sinai have a total sinistral offset of about 22 km and the two largest sinistral displacements in Saudi Arabia total 8 km of offset. The surface expressions of these major faults are linear open wadis, usually without any outcrop of the faults, the presence of which is demonstrated by dissimilar geology on either side of each wadi (Fig. 12). A minimum figure for the vertical component of shoulder uplift is obtained from the maximum topographic height of the uplifted fault-bounded Precambrian block. Precambrian peaks inland of the coast have been uplifted higher than the Cambrian penepain on

which the Cambro-Ordovician Saq sandstone of the Cover Rocks lies. The greatest preserved shoulder uplift is 2,580 m on Jabal Lawz.

Two fault plane solutions for the November 22, 1995 magnitude 7.3 earthquake calculated by Harvard University and the National Earthquake Information Center of the USA both indicate a north-northeast fault plane and a sinistral displacement. The zone of epicentral rupture on the Saudi Arabian shore showed the shoreline unchanged, but open fault planes where the land was shoulder uplifted in steps with an accumulated total of 90 cm of uplift (Roobol et al. 1999).

The age of the Aqaba fault system is younger Cenozoic or Neogene, being younger than 20 Ma and resulted from the second stage of opening of the Red Sea. Stage one opening is preserved in the Gulf of Suez but an additional 115 km of sinistral displacement has widened the northern part of the Red Sea trough.

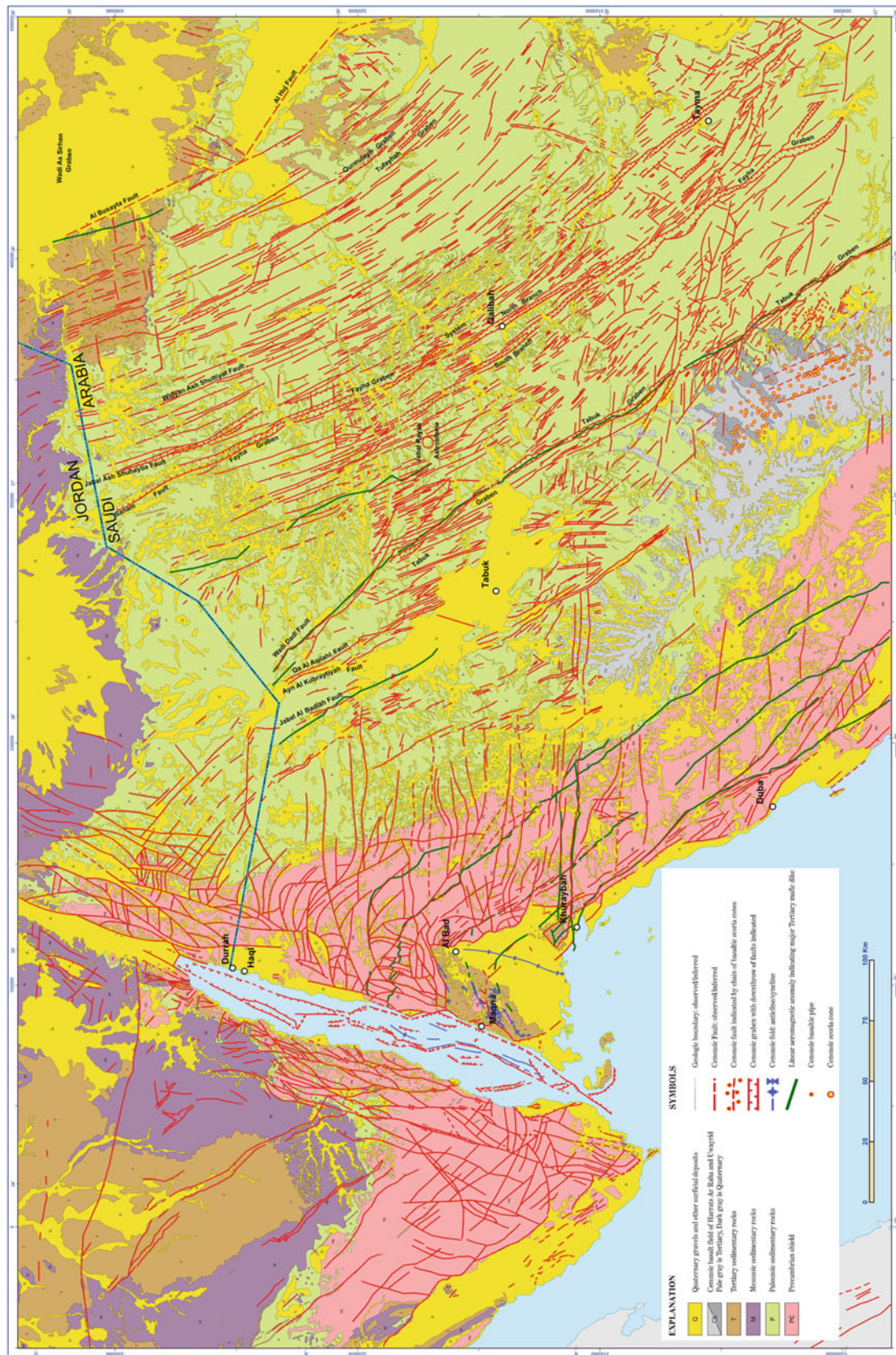


Fig. 11 Cenozoic faults and folds of northwest Saudi Arabia and adjacent areas shown on a geological base map simplified after Clark (1987), Davies and Grainger (1985), Grainger and Hamif (1989), Janjou et al. (1996, 1997), Rowaihy (1985), Vastlet et al. (1994), and Wallace et al. (2000a, 2000b, 2001)



Fig. 12 View looking south along a prominent north-northeast fault (Gulf of Aqaba system) cutting the Cambro-Ordovician Saq sandstone on the Haql to Tabuk road at 28°51.990'N, 35°33.463'E. The block on

the right (west) is downthrown at least 70 m whereas Precambrian basement is exposed under the sandstone of the other block

6 A Zone of Intense Deformation Along the Eastern Margin of the Gulf of Aqaba

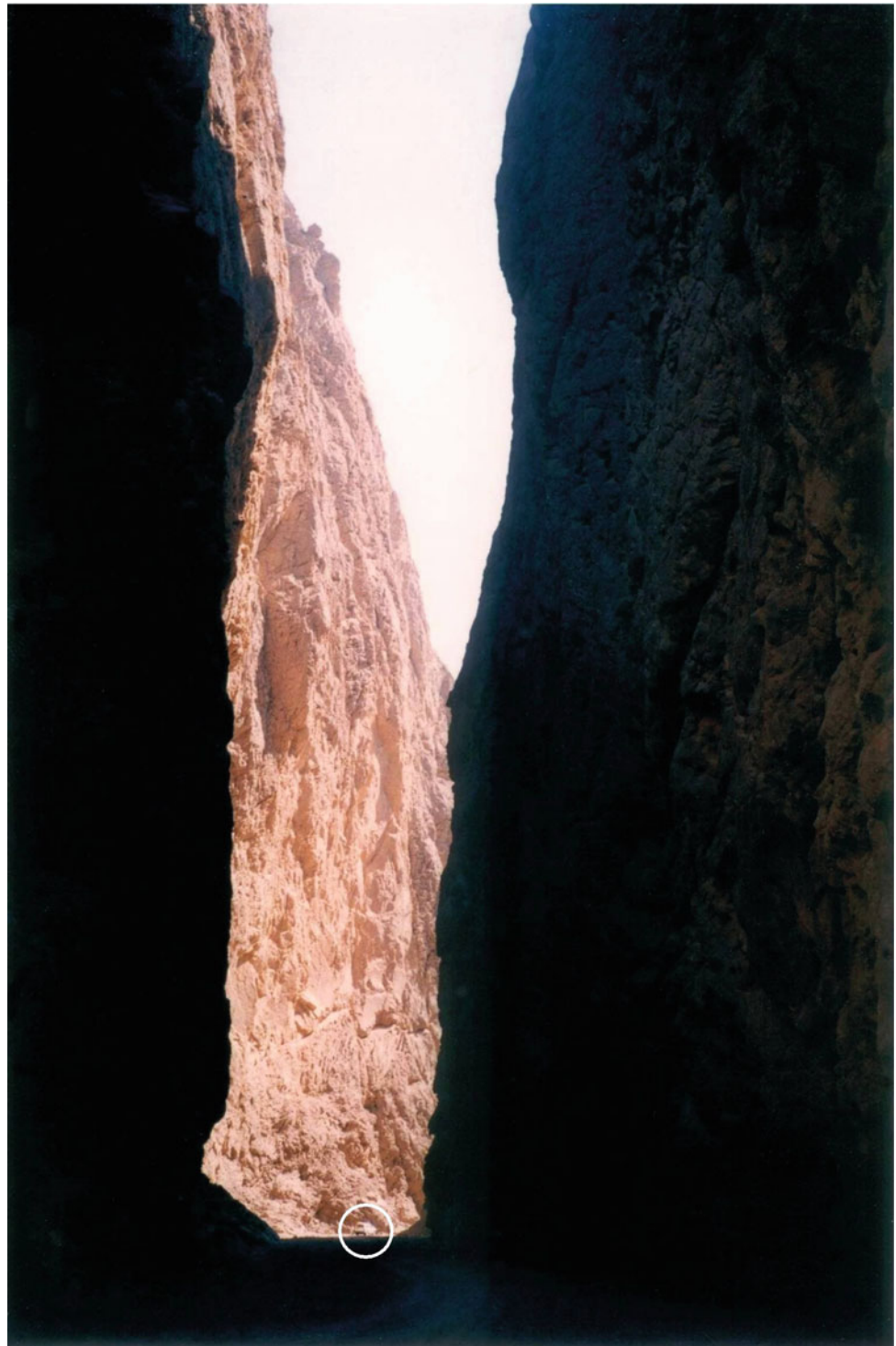
A major feature that was previously undescribed on the eastern side of the Gulf of Aqaba in Saudi Arabia is a belt extending for up to 25 km inland where many granite plutons are shattered with cataclastic zones of finely crushed rock. In Wadi Mabrak (along the Jordan border) at a distance of 18 km from the coast the shattered zone is 20 km wide. The shattering is best noticed in the granite plutons which have an uncharacteristic very crumbly type of erosion in which rock pinnacles rise from scree covered slopes. Erosion produced vertical gorges through the shattered granite which erodes similarly to sandstone. The best example of such a gorge in shattered granite is that of Tayyib al Ism (Fig. 13). The belt of shattered granite plutons and their debris curtains can be recognized on Landsat images and differs from the

normal blocky weathering of granite plutons further east and throughout the Arabian shield.

During fieldwork over two seasons, it was found that in some areas of steep cliffs along the coastline parts of the road maintained by the Saudi Arabian Border Patrol were incomplete along the section of shattered granites immediately adjacent to the Aragonese Deep. Here, the high granite cliffs plunge down directly into the Deep, which has a maximum depth of 1800 m. Along this coastal section, cliff collapses are frequent and the road is constantly being renewed.

Whereas the granites in a belt 25 km wide along the eastern shore of the Gulf of Aqaba are shattered, the associated rocks are intensely faulted. The latter comprise Tertiary sedimentary rocks of the Maqna block along the southern shoreline of the Gulf of Aqaba and the metavolcanic-sedimentary rocks of the Precambrian shield along the northern shoreline. Both types of rock are intensely

Fig. 13 The gorge of Tayyib al Ism. This vertical walled gorge is cut into shattered granite with cataclastic zones of crushed rock adjacent to the Gulf of Aqaba (note the Toyota Landcruiser for scale, circled). The location is latitude 28°33'35.74"N, longitude 34°48'09.98"E



faulted and the belt of intense faulting extends beyond the belt of shattered granites for a distance of 50 km from the coast. Immediately adjacent to the coastline, the Tertiary sedimentary rocks are cut by numerous small faults with spacings of only a few metres and vertical displacements of

centimetres to metres (Figs. 14 and 15). In the Precambrian shield along the northern shores some indication of this coastal intense faulting can be obtained from the 1:100,000 WSA aerial photomosaics where the larger faults have been traced, and a section of this fault map is recorded in Fig. 16.

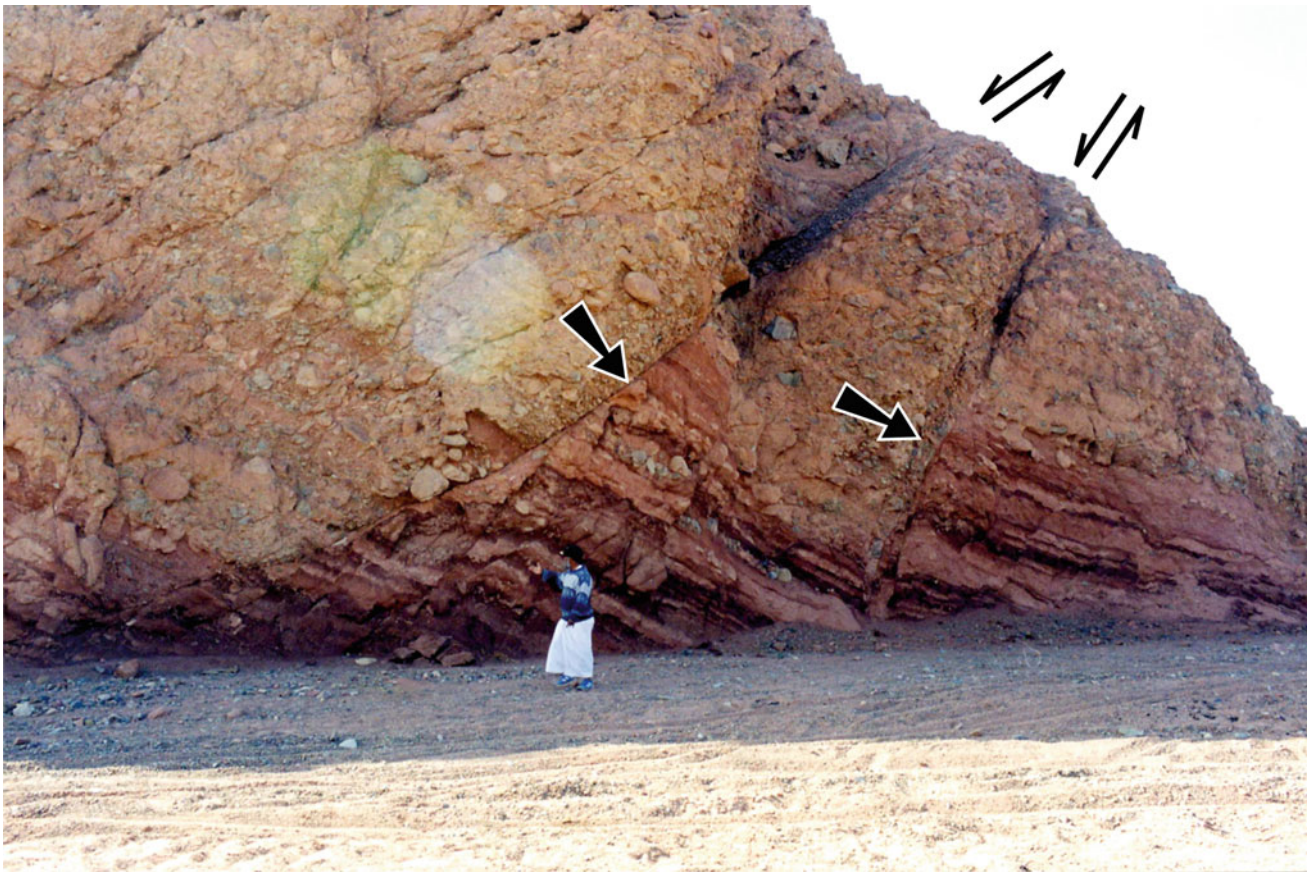


Fig. 14 The Oligocene Sharik formation sediment in Wadi Sukk showing numerous small faults typical of the coastal belt along the Gulf of Aqaba. Two of the main faults and their sense of motion are

indicated by arrows. Looking south with the Gulf to right at latitude $28^{\circ}31'15.7''N$, longitude $34^{\circ}49'21.7''E$

7 A Major Fold Structure to the East of the Gulf of Aqaba

Within a 50-km wide belt adjacent to the Gulf of Aqaba, which includes the 25-km wide zone of coastal shattered granite, the rock units of the Precambrian shield form a broad fold having the appearance of a drag fold consistent with the sinistral displacement of the Gulf of Aqaba (Figs. 6 and 7). This fold affects the Precambrian rock units of northwest Saudi Arabia as well as the many Precambrian dikes contained within them. When the structure is traced from east to west toward the Gulf of Aqaba, inland north-west trends become east-west oriented and then turn to northeast-southwest adjacent to the Gulf. This structure can be seen on Landsat and Google Earth images but no similar structure can be seen on the Sinai side of the Gulf. The fold structure was first recognized by Clark (1987) when he mapped the Al Bad 1:250,000 quadrangle, but no comment was made on the age of the structure. A clear case can be made that this fold, including the rotation of Precambrian rock units, Precambrian dikes and Tertiary dikes, is of

Cenozoic age corresponding to the second stage of opening of the Red Sea. Although the structure resembles a drag fold resulting from the sinistral displacement along the Gulf of Aqaba, the absence of a similar structure on the Sinai side does not support this interpretation. Rather a different origin is indicated, namely that the 50-km wide fold structure formed before the main transform faulting and pull-apart basin formation along the Gulf of Aqaba. That is, the second stage of opening of the Red sea was accommodated at first by folding, then by the production of a shatter zone and belt of intense local faulting and finally by pull-apart basins related to large movements on a small number of faults. Thus, rather than being a simple drag fold, the structure records the earliest sinistral displacement of the Arabian Plate from Sinai. Later, a belt of north-northeast faults of the Gulf of Aqaba system formed over a broad zone with individual sinistral displacements of up to 9 km. Finally, major displacement on a few of these faults led to the formation of pull-apart basins. This later displacement resulted in separation of the entire fold structure which is now preserved intact within the Arabian Plate in Saudi Arabia.



Fig. 15 Miocene Nutaysh formation sediment on the coast immediately south of Maqna showing numerous small faults typical of the coastal belt along the Gulf of Aqaba. The location is latitude 28°23'27.93"N, longitude 34°44'13.67"E

Another indication of the age of the fold structure is obtained from the fact that the Precambrian lithologies and dikes were rotated through 90 degrees anticlockwise to form the fold. However, the aeromagnetic traces of the major gabbro dikes that parallel the margins of the Red Sea are rotated through only about 45 degrees in an anticlockwise direction. This suggests that they were emplaced well after the fold structure started to form. Although poorly exposed, these dikes have a range in ages of 24 to 22 Ma (cf. Table 1 in Bosworth 2015) which dates the latter part of the folding.

8 Arcuate Faults and Offset of Tertiary Gabbro Dikes

The 50-km wide fold structure adjacent to the Gulf of Aqaba within Saudi Arabia shows a number of arcuate faults that parallel the deformed Precambrian lithologic units and include Precambrian dikes (Figs. 6 and 7). These structures are Precambrian faults that have also been deformed by the major fold structure. Originally the Precambrian faults were planar with linear surface traces but they were reactivated in

Neogene time as part of the fold structure and became arcuate. This can be demonstrated because of the presence of thick gabbro dikes that occupy Tertiary pre-rift faults that parallel the entire length of the Red Sea coast. The dikes were first described by Blank (1977; Plate 3 therein), Blank and Andreasen (1991) and Johnson and Vranas (1992), and are particularly prominent on the aeromagnetic map of Saudi Arabia (Zahran et al. 2003). These dikes are rarely exposed at the surface (Fig. 17), where they are usually 200 to 300 m thick and nearly vertical. $^{40}\text{Ar}/^{39}\text{Ar}$ ages show the dikes to have formed mainly from 24 to 22 Ma (Bosworth 2015). The northwesterly-trending Tabuk graben, a youthful morphologic structure, can be traced right across the study area (Fig. 7) and aeromagnetic data show it to be underlain by a Tertiary gabbro dike (which is a prominent linear feature across the centre of Fig. 6) that has been named the Great Ja'adah Dike (Phoenix Corporation 1985). Conversely the aeromagnetic data also show that the parallel Fayha graben and another unnamed graben further to the east are not underlain by gabbro dikes. As the aeromagnetic traces of the dikes are followed into the 50-km wide fold structure alongside the Gulf, they can also be seen to be rotated. One

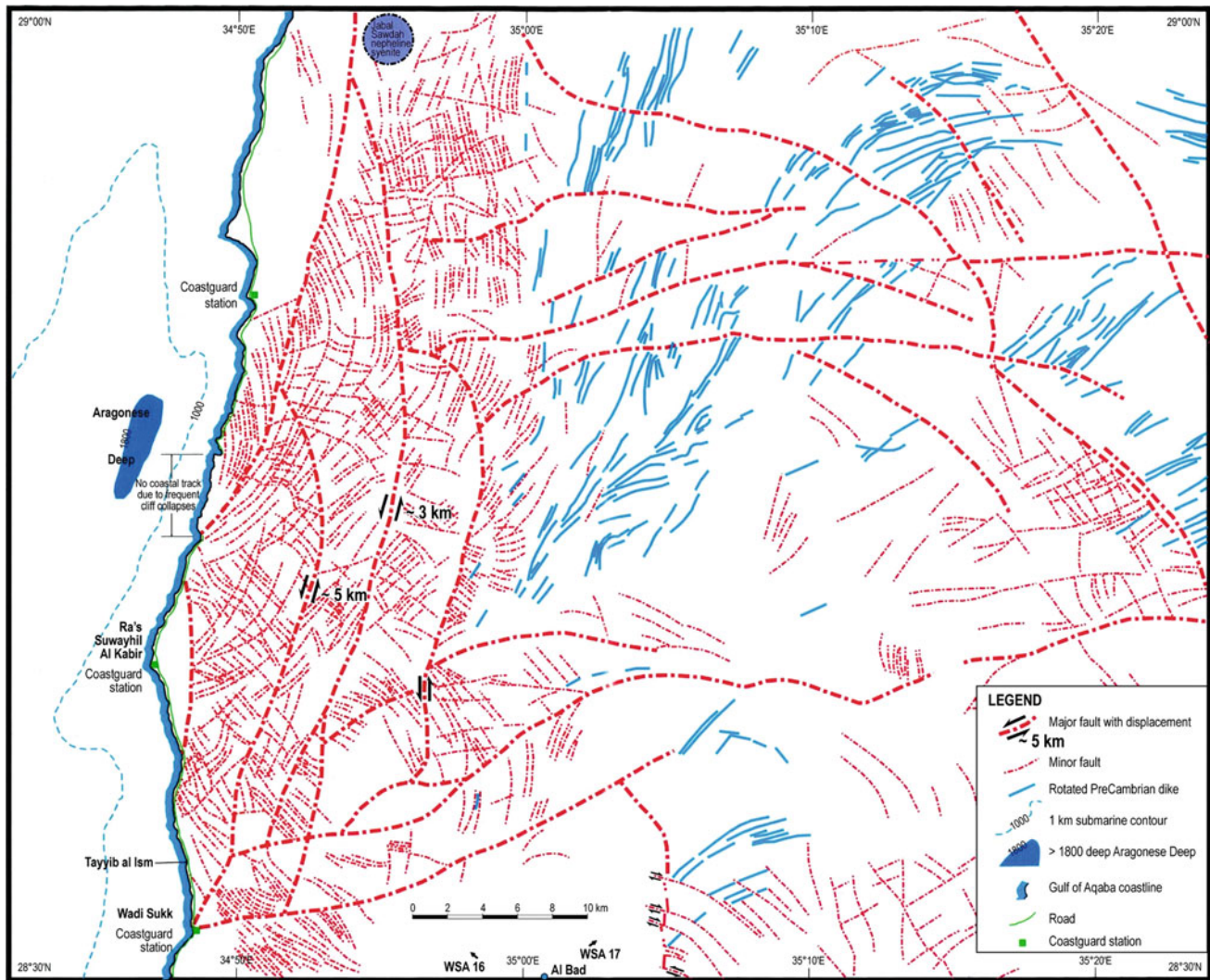


Fig. 16 Fracture pattern and rotated Precambrian dikes on the east side of the Gulf of Aqaba

of them can be traced in detail through the zone of intense faulting (Fig. 18). More detail of the fault-dike relationship is shown in Fig. 7. Thus, the age of the major fold structure, and the arcuate nature of the Precambrian faults is demonstrated to be Neogene in age or in part younger than the gabbro dikes at about 24–20 Ma, which corresponds to the second stage of opening of the Red Sea. It should be noted that the curvature of the trace of the gabbro dikes is less arcuate than that of the structural trends in the Precambrian shield, because the Tertiary dikes probably were emplaced after the folding had started.

We have been unable to locate aeromagnetic data for the Sinai Peninsula, but youthful graben structures parallel to those in northwest Saudi Arabia exist there and some are underlain by Tertiary gabbro dikes as described by Eyal et al. (1981).

9 Cenozoic Reactivation of a Precambrian East-West Fault System

East-west faults form a well-developed Precambrian fault system that is present throughout the Arabian shield. In the Gulf of Aqaba region faults of this system were reactivated during the Cenozoic to form a belt between the Aqaba fault system and the Ribbon fault system. Some of these faults can be traced to the west where they become arcuate faults within the major fold structure. Others cut the Phanerozoic sedimentary rocks and some cut and down-drop the Phanerozoic Cover Rocks of northwest Saudi Arabia as blocks and grabens into the Precambrian Shield. Figure 19 shows one of these deeply-eroded faults (near the village of Shigri, after which it is here named) that can be traced for 150 km (cf. Fig. 7). At its

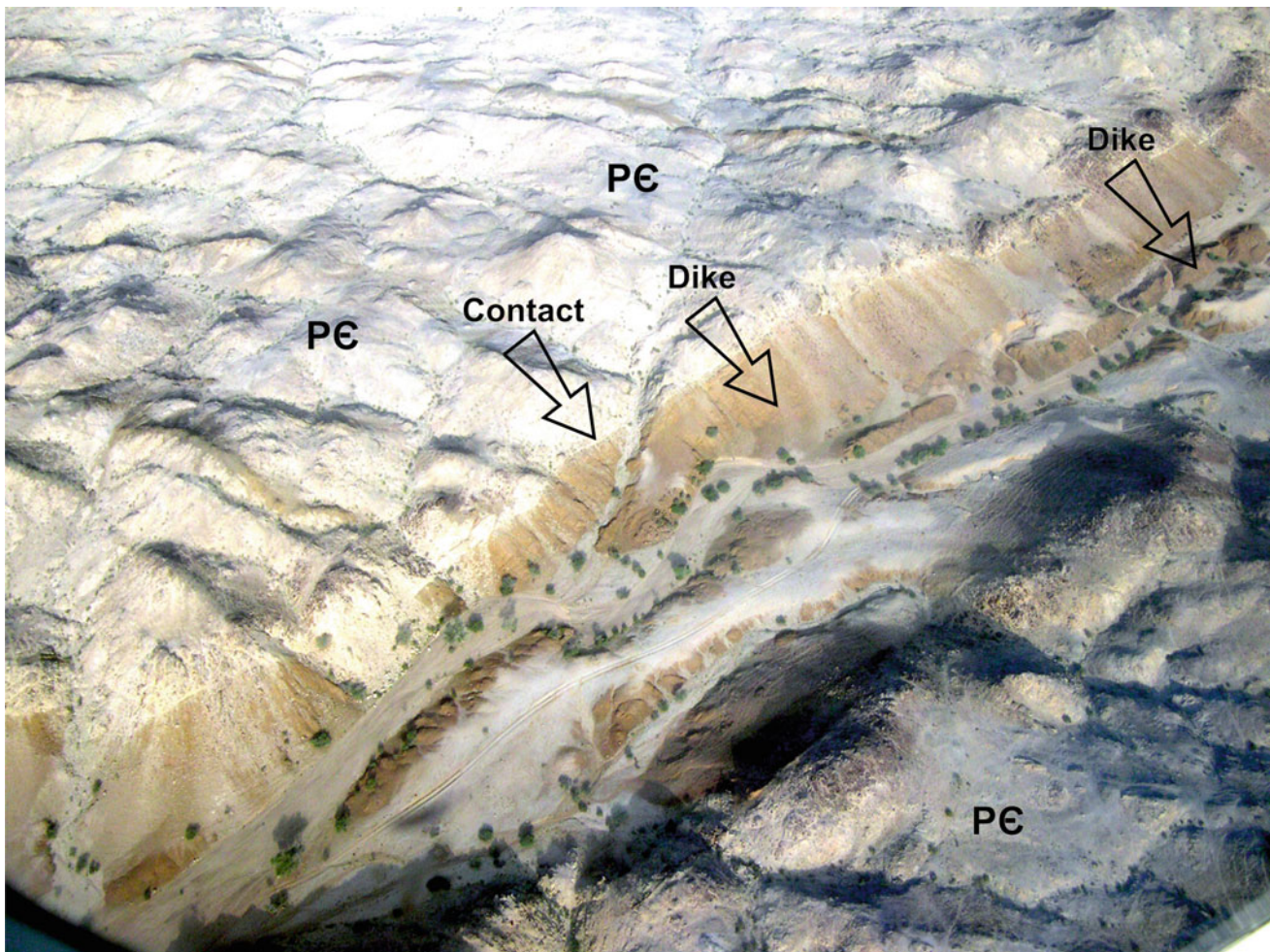


Fig. 17 Tertiary gabbro dike exposed near coastline near Duba. These dikes are seldom exposed at the surface but have very strong aeromagnetic signatures. The dike forms the dark-coloured walls of

the wadi and has a sharp contact with the country rock. The location is latitude 27°28'29.16"N, longitude 35°45'46.68"E

western end on the Red Sea coast near the village of Khuraybah (Fig. 7) the fault scarp is mantled in Lower Miocene Raghama reef facies limestone. In its central part to the west of the Duba-Tabuk road the fault is represented by a deep erosional canyon cutting through the Phanerozoic Cover Rocks (Saq Sandstone) and deep into the Precambrian basement. The Saq Sandstone is offset across this fault (Fig. 19). At its eastern end the fault appears to cut Tertiary basalts of Harrat Ar Raha (Fig. 7). Much of this fault is underlain by an aeromagnetic anomaly indicating the subsurface presence of a major gabbro dike. Another prominent east-west fault in the Khuraybah area had its westernmost end reactivated in Cenozoic times because it truncates and down-drops a block of Lower Miocene Raghama limestone that can be seen adjacent to the coast road.

Some of the east-west faults are accompanied by aeromagnetic anomalies that are thought to represent Tertiary gabbro dikes. East-west aeromagnetic anomalies occur on Harrat Lunayyir where they are associated with Quaternary chains of basaltic scoria cones. These relations suggest that

the east-west faults were reactivated in both pre-and syn-Red Sea rift times.

10 The North-Northwest Red Sea Coastal Fault System

The broad coastal plain that borders the Red Sea obscures the Precambrian shield but seismic refraction profiles show that the 40-km thick Precambrian Shield (Gettings et al. 1986) thins to about 15 km beneath the coastal plain (Makris et al. 1983), as is also indicated by gravity data. The thinning of the Precambrian shield to around 15 km is believed (from mapping the coast plain elsewhere, e.g. Roobol and Kadi 2008), to be achieved by normal faulting. The faults strike parallel to the Red Sea and comprise the north-northwest Red Sea coastal fault system. Roobol and Kadi (2008) were able to subdivide the fault system into two distinct ages corresponding with pre-and syn-rift stages

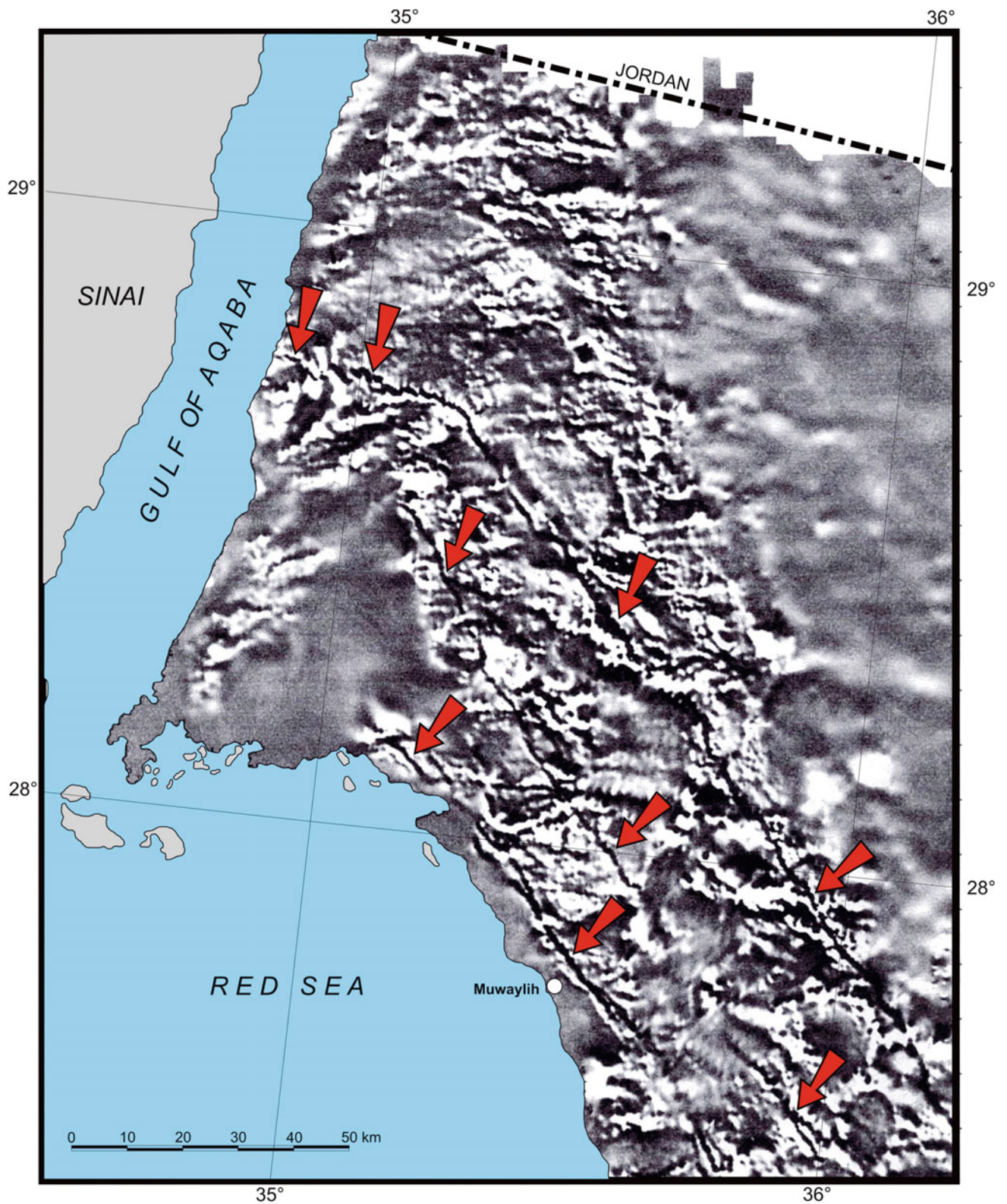


Fig. 18 Detail showing curved aeromagnetic traces of hidden gabbro dikes (indicated by red arrows) through the zone of intense faulting immediately adjacent to the Gulf of Aqaba. The relationships of the most prominent dikes to the Cenozoic faults are shown in Fig. 7



Fig. 19 Part of the 150 km long east-west fault eroded into a deep canyon near the Duba-Tabuk road north of Shigri village at latitude $28^{\circ}03'34.6''\text{N}$, longitude $35^{\circ}55'58.8''\text{E}$. There is a small downthrow of the Cambro-Ordovician cover to the north (right)

of the opening of the Red Sea. First the Afro-Arabian shield was attenuated in pre-rift times to form a “Pre-rift Foothills Normal Fault System”. These faults are inclined steeply both toward and away from the Red Sea and create a horst and graben topography that has not yet been removed by erosion. This fault set is distinct because many of the faults contain major Tertiary gabbro dikes with distinctive aeromagnetic signatures. A later set formed as a result of the Stage 1 opening of the Red Sea. This later set, also parallel to the Red Sea coast, was named “The Red Sea Coast Plain Fault System”. The faults are syn-rift rotational normal faults (see cross section in Roobol and Kadi 2008) and are believed to result from gravity collapse of the Precambrian shield along the margins of the newly-opened Red Sea. In northwestern Saudi Arabia only one of these younger faults is visible as the Master Listric Fault behind the Red Sea coastal plain. This is a prominent but deeply-eroded fault scarp separating the coast plain from the Precambrian shield.

The north-northwest Red Sea Coastal fault system can be traced along the entire length of the Red Sea and locally shows Tertiary base metal mineralization described by Hayes et al. (2002). A similar fault system exists on the African side of the Red Sea and can be seen on Landsat and Google Earth images.

11 The Ribbon Fault System

East of longitude 36°E , both the Gulf of Aqaba and the east-west fault systems die out and are replaced by a different fault system named here the Ribbon fault system. This is a belt of normal faults 250 km wide that trends north-northwest in the north and arcs around to northwest in the south of the map area (Fig. 7). The eastern limit of this fault system has been documented at longitude 38°E in the Sirhan-Turayf Basin 1:250,000 sheet (Johnson, unpublished 2007). On the map (Fig. 7) approximately 2,400 of these



Fig. 20 Google Earth image showing ribbon faults in the Marthoum area. Chains of elliptical columnar-jointed basalt pipes have been emplaced along the faults. Horst blocks are marked “h” and grabens “g”. The width of the field of view is approximately 9.4 km

faults are shown and these can all be seen on the SRTM image. However, in the field, the faults are much more numerous and only about a third (the longest and most prominent ones) are shown in Fig. 7. Minor faults can be seen on Google Earth images and they are particularly prominent in the field where they divide the Phanerozoic sandstones into long narrow horst-graben strips with topographic differences of up to 4 m. These faults are a swarm and are named “Ribbon faults” because they cut up the rocks into long ribbon-like strips. They are of small displacement with fault scarps seldom more than 3 m high. In many places the faults are distinct as they are filled with iron oxide/hydroxide that resists erosion to form ridges. In some cases there are open fissures with little apparent vertical displacement. In all cases, however, these faults and fissures appear to result from crustal extension.

An example of ribbon faulting in the Marthoum area of the Tayma quadrangle (Vaslet et al. 1994) is shown in a Google Earth image in Fig. 20 at latitude 27°15’N, longitude 37°50’E. The ribbon faults are apparent as sand and gravel filled grabens (marked as “g” in the diagrams) separated by hummocky sandstone horsts (marked as “h”) with a light colour of wind-blown sand. The faults are marked by chains of Saq Sandstone hills that have joints filled with limonite ironstone (due to weathering of mafic minerals in the sandstone) that resists erosion (Fig. 21). In this area between the Tabuk graben to the east and Harrat Uwayrid to the west there are 100 Tertiary basalt pipes (Liddicoat 1982) that are intruded along the ribbon faults and occur in chains. Individual pipes are lenticular along the host ribbon fault (Fig. 20).

Ribbon faults are particularly striking in an area of Devonian Tawil Sandstone in the Thaniyat-Turayf



Fig. 21 Line of limonitized Wajid sandstone hills along a Cenozoic ribbon fault in the Marthoum area at latitude 27°14'36.75"N, longitude 37°48'42.29"E

Fig. 22 Google Earth image of ribbon faults in the Devonian Tawil formation sandstone at latitude 29°30'N, longitude 37°45'E. The faults are represented by linear chains of limonitized sandstone caused by weathering of the rocks and migration of limonite into the fault zone. The width of the field of view is approximately 7.8 km

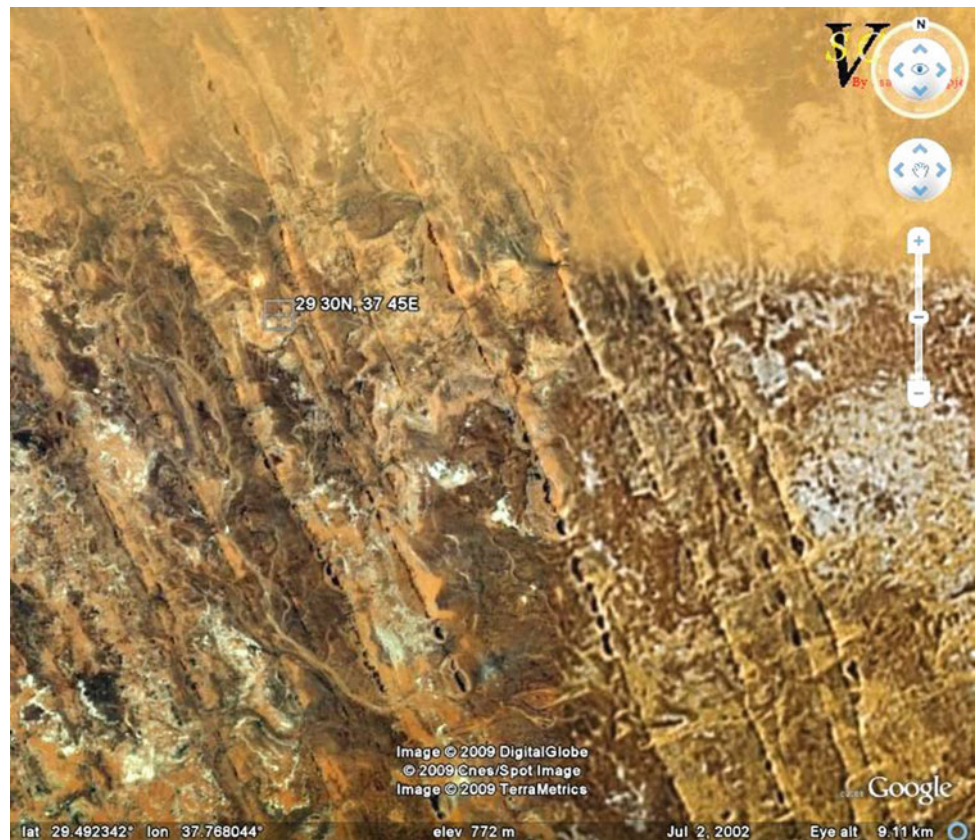




Fig. 23 Line of limonitized Devonian Tawil sandstone hills along a Cenozoic ribbon fault. Behind the line of hills, the sandstone is exposed in a low horst block. In the foreground the sandstone has subsided in a

graben now largely filled with dark gravel of ferruginated sandstone. The location is latitude 29°06'14.15"N, longitude 37°45'44.87"E

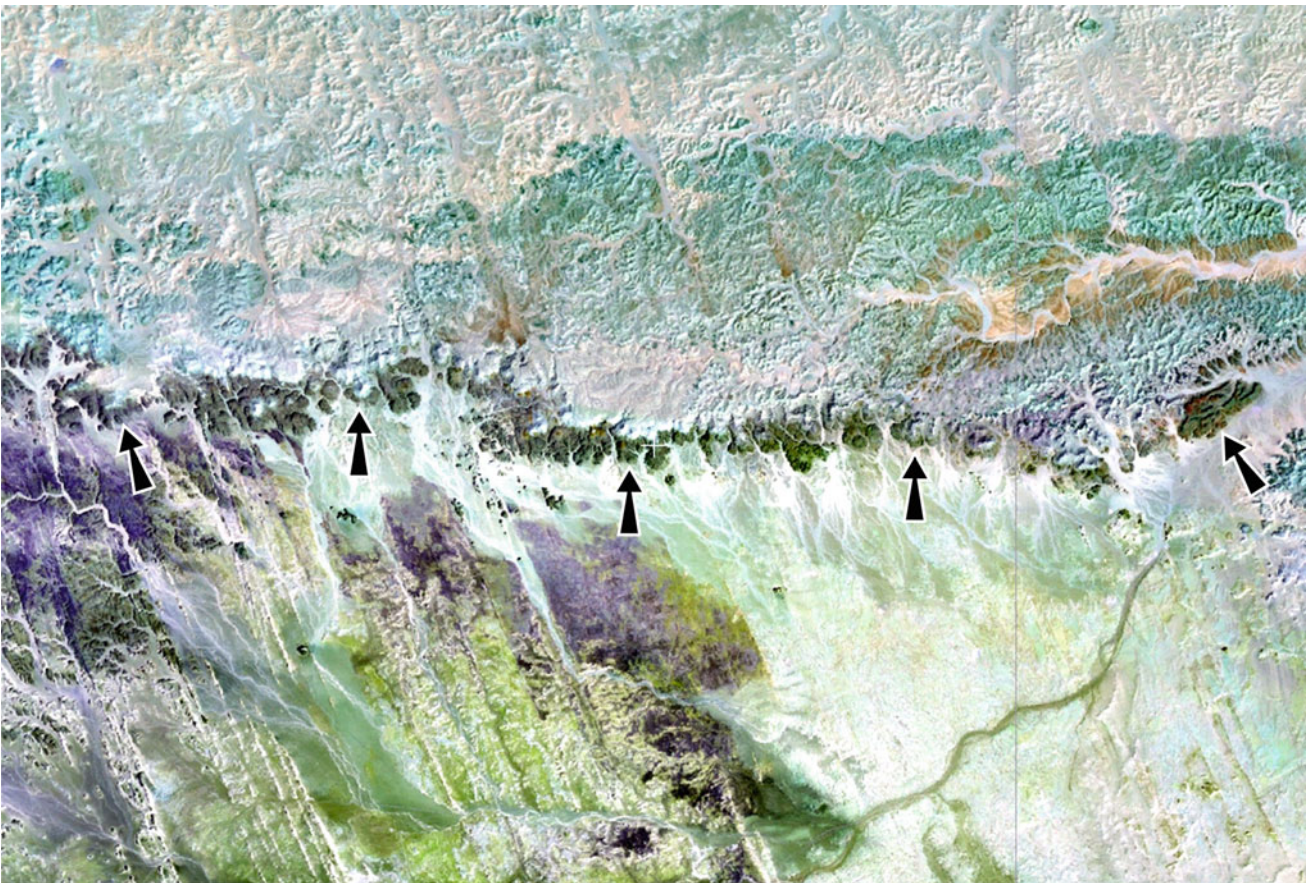


Fig. 24 NASA World Wind pseudocolour image of the Thaniyat-Turayf escarpment. The Devonian Tawil sandstone formation is exposed in the southern half of the image and includes the dark rocks (indicated by the arrows) along the base of the escarpment. In the north the sandstone is overlain by a thin layer of Cretaceous Aruma

Group. The white coloured sediments in the top half of the image are the Tertiary Turayf Group, and all can be seen to be cut by the ribbon faults which are therefore Cenozoic in age. The width of the field of view is approximately 47.7 km

quadrangle (Wallace et al. 2000a). Here long thin strips of rock bounded by ribbon faults can be seen where light coloured sandstone horst blocks stand above dark-coloured

gravel-filled grabens. Some of the ribbon faults are exposed as fault scarps up to 3 m high along which yellow wind-blown sand is banked.

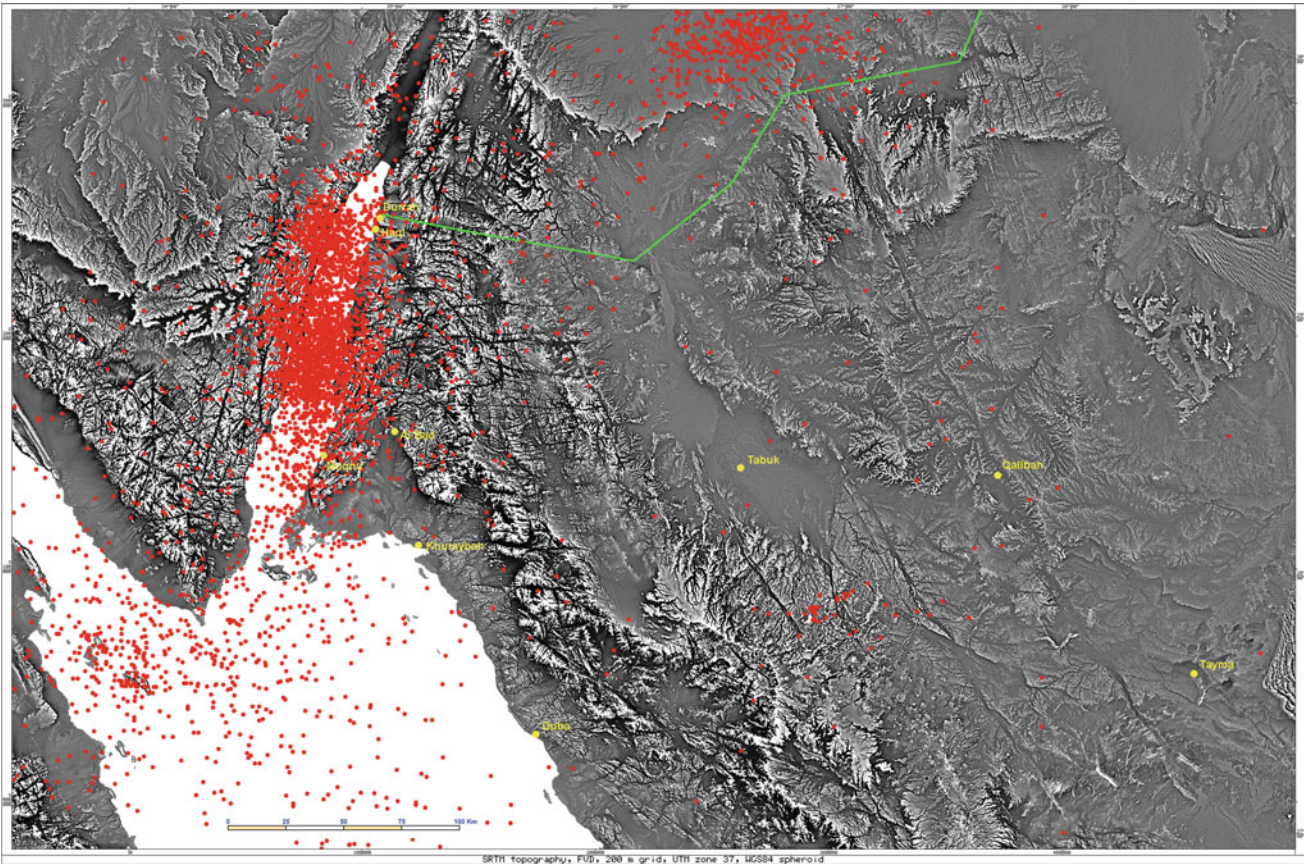


Fig. 25 SRTM surface elevation, First Vertical Derivative, showing earthquake epicentres greater than magnitude 3 for northwest Saudi Arabia and adjacent areas

To the north of the location in Fig. 20 in an area of spectacularly beautiful desert scenery are areas of ribbon faulting that appear truly remarkable on Google Earth images. The faults themselves are marked by straight lines of sandstone hills bounded by joints filled with limonite. An example at about latitude $29^{\circ}30'N$, longitude $37^{\circ}45'E$ is shown in Fig. 22. A field photograph taken in a traverse through the area is shown in Fig. 23. The desert tracks mainly follow the grabens because they are infilled with brown limonitized fragments derived by erosion of the limonitized ironstone fill of the ribbon faults. In contrast, the sandstone horsts form light coloured hummocky ground where yellow wind-blown sand has gathered.

Evidence for the Cenozoic age of the ribbon faults is found in an area of Mesozoic and Tertiary sedimentary rocks exposed in the Thaniyat-Turayf quadrangle (Wallace et al. 2000a). The area is well known because of the prominent Thaniyat-Turayf escarpment showing the Devonian Tawil sandstone formation in the lower part, unconformably overlain by Cretaceous Aruma Group, and in turn unconformably overlain by the Tertiary Turayf Group. The latter is well known for the two phosphorite members and a USGS adit into the lower part of the Thaniyat phosphorite member.

Wallace et al. (2000a) are non-committal on the age of the faults but the Geocover 2000 images from NASA World Wind (Fig. 24) and a field visit clearly indicate that some ribbon faults cut all members especially the Tertiary sediments, indicating that they are Cenozoic faults. A small number of faults in the area may be Pre-Cretaceous in age as Wallace et al. (2000a) show one such fault on their map.

12 Recent Seismicity

Earthquake epicentres from 1950 up to 2015 taken from the Saudi Geological Survey database were plotted on the FVD images of the SRTM topography for possible correlation with mapped fault trends. The seismic hazard for the Red Sea, the Gulf of Aqaba and western Saudi Arabia is discussed by Stewart (2007) and Zahran et al. (2015, 2016), and hazard estimates for the Sinai area are also given by Sawires et al. (2016). The epicentres are plotted as red dots on the same base map as shown in Fig. 5, with 5007 events above magnitude 3 shown in Fig. 25, and 986 events greater than magnitude 4 shown in Fig. 26. Earthquakes larger than magnitude 4 are presumably reasonably well located

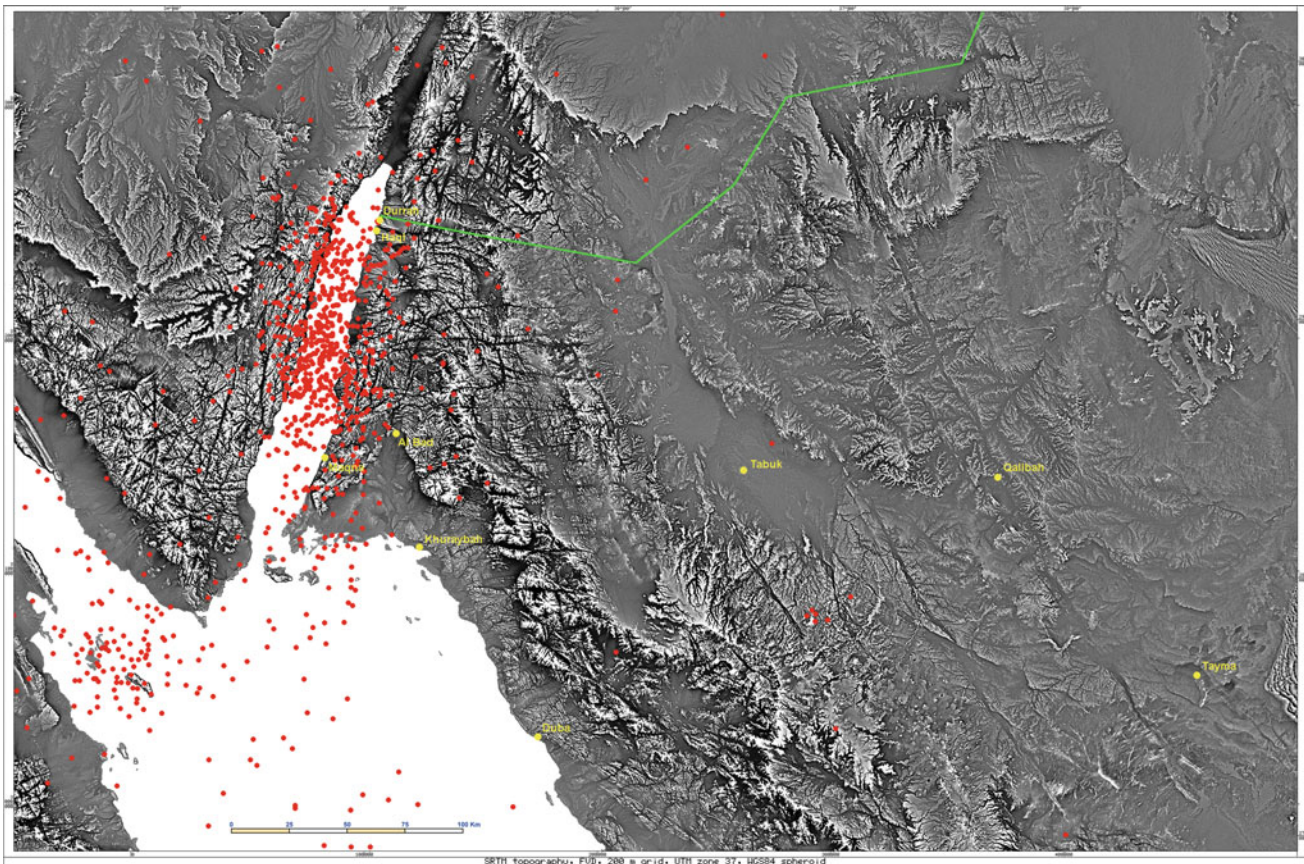


Fig. 26 SRTM surface elevation, First Vertical Derivative, showing earthquake epicentres greater than magnitude 4 for northwest Saudi Arabia and adjacent areas

(probably to within 10 km) and should exclude most events of cultural origin such as quarry blasts. The large cluster of events near the centre of the upper margin of Fig. 25, between 36°E and 37°E in fact probably represents activity related to phosphate mining rather than naturally occurring earthquakes, and is absent in Fig. 26. The earthquake activity extends onshore on both sides of the Gulf, and the seismicity in the Sinai Peninsula is discussed by Abdel-Rahman et al. (2009). A more complete epicentre plot, especially for the region of the Dead Sea Transform to the north of the Gulf of Aqaba, has recently been presented by Wetzler and Kurzon (2016), and the seismicity of the northern Red Sea in particular has also recently been discussed by Mitchell and Stewart (2018).

The spatial variation in earthquake activity can also be shown by the rate of release of seismic moment, which for an earthquake is the product of fault plane area, the fault slip or displacement and the shear modulus of the rock, and is probably the most physically realistic measure of the size of an earthquake. Using earthquakes greater than magnitude 4 since 1950, the logarithm of the cumulative seismic moment in 5 km cells (in units of N m) is shown in Fig. 27.

The Arava (Arava) Fault section of the Dead Sea Rift from about 29.5°N northward (between the Gulf of Aqaba and the Dead Sea) shows relatively low seismicity compared to adjacent sections of the rift zone (Ben-Menahem and Aboodi 1981), and the southern end of the Gulf of Aqaba currently also has relatively low activity. These two zones may only be temporarily quiescent, and could in fact represent areas with relatively high earthquake risk, illustrating the problem in estimating hazard from incomplete data sets. Klinger et al. (2000b) also suggest that historically there have been fewer large earthquakes than expected along the Arava Valley in Jordan, although much of the observed rate of movement could be accommodated by an M_w 7.6 event about every 6000 years. Paleoseismic studies along the southern Dead Sea fault show that the return intervals of large earthquakes over the past 5000 years are very variable, with long periods of relative quiescence (Klinger et al. 2015), which illustrates the difficulty in determining the long-term seismicity and risk from instrumental data recorded over only a few tens of years. Presumably the average left lateral rate of movement in the southern Gulf of Aqaba and near the Tiran Strait is similar to that further north (about

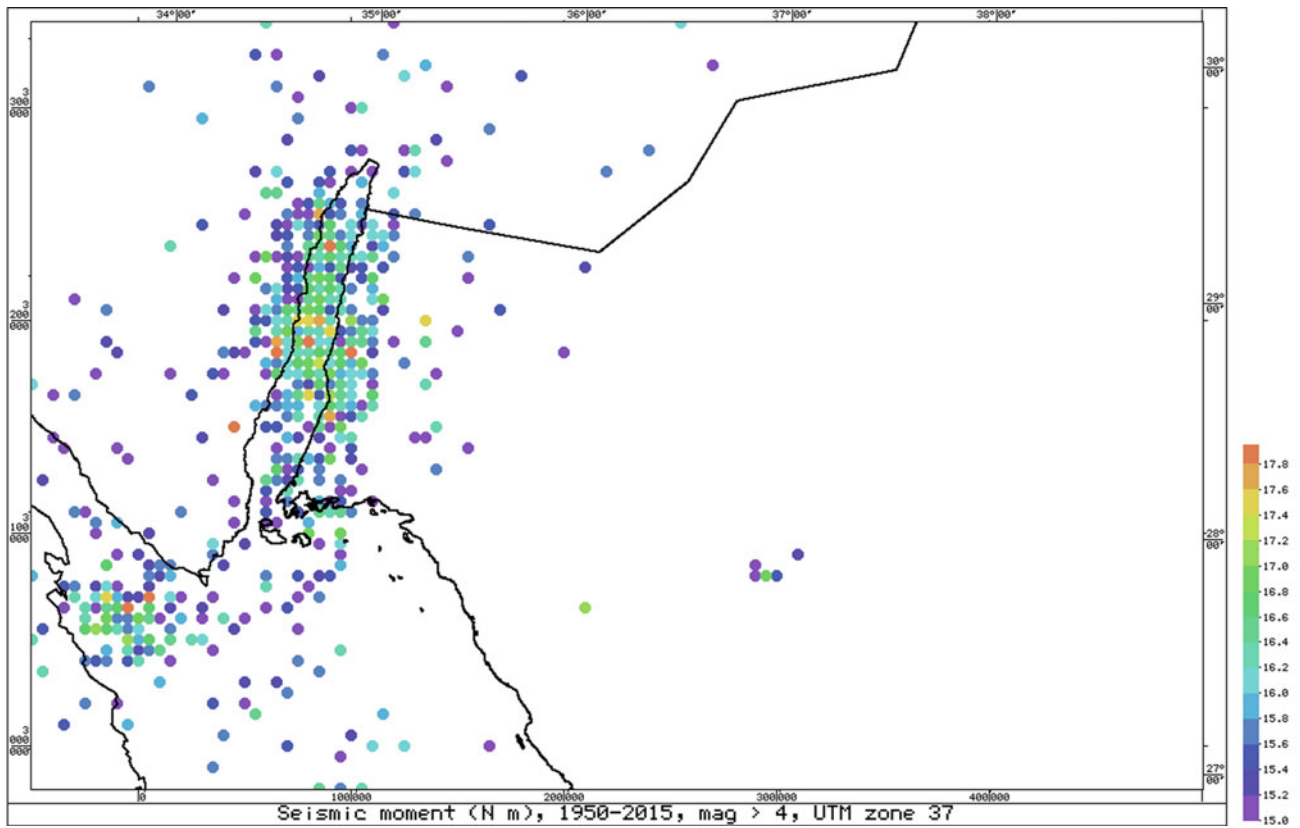
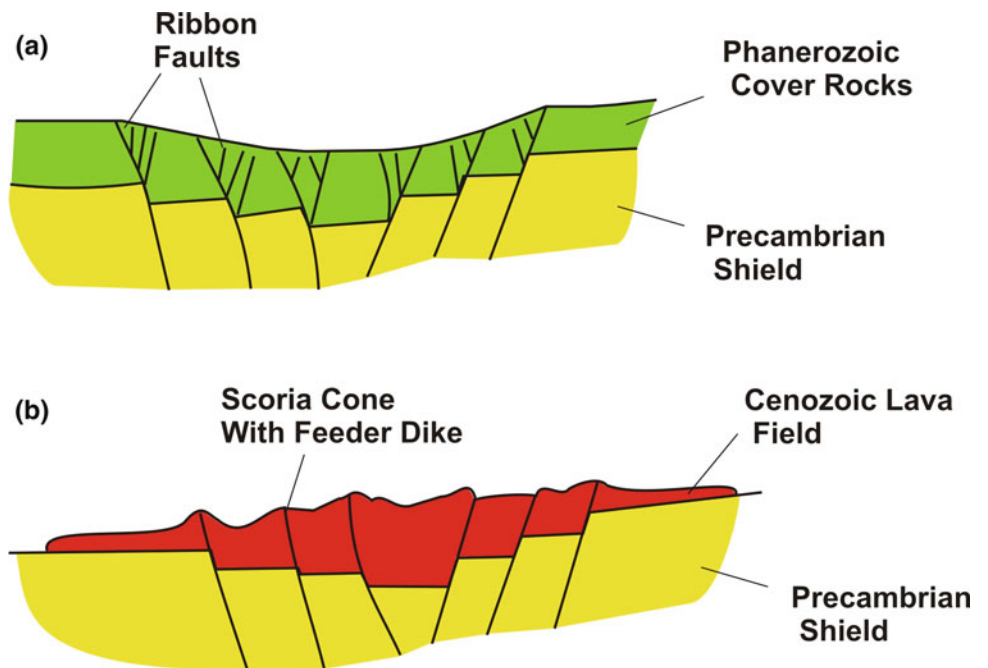


Fig. 27 Earthquake seismic moment (a measure of energy release, in N m units) summed over 5 km cells using seismicity data from 1950 to 2010 and events greater than magnitude 4

Fig. 28 Diagram that illustrates a possible explanation for the two types of crustal extension along the western side of the Arabian Plate. In the north in the unmetamorphosed sedimentary cover rocks the faults feather to form a wide belt of ribbon faults (a). At depth the crystalline basement of the Precambrian shield forms a simple graben as found along the Makkah-Madinah-Nafud volcanic line (b)



5 mm/year) so there may be an appreciable risk of damaging earthquakes that could affect any planned infrastructure despite the current moderate seismicity in this area.

The epicentres plotted on the SRTM images are likely to be in error by at least several km, and hence it is difficult to correlate the activity with any particular mapped fault. As expected, most of the seismic activity lies within and on the margins of the Gulf of Aqaba, along which most movement occurs. Even if the epicentres and focal depths were known precisely, correlation of events with known faults may be difficult except for very shallow earthquakes since most faults are not vertical. However, the seismicity does show the areas that are currently undergoing movement, but this does not show the longer-term changes over a geologic timeframe.

13 Discussion

The thousands of Cenozoic faults in NW Saudi Arabia record a tectonic history that extends to at least 25 Ma. Roobol and Kadi (2008) were able to subdivide the faults parallel to the Red Sea coast into two distinct age groups, pre-rift and syn-rift relative to the opening of the Red Sea. The oldest pre-rift faults are those parallel to the Red Sea, some of which the aeromagnetic maps show to host major gabbro dikes. Most prominent of these is the Tabuk graben which is underlain by the Great Ja'adah Dike. These dikes (which rarely outcrop at the surface) have recently had their age range revised to 24–22 Ma by $^{40}\text{Ar}/^{39}\text{Ar}$ dating (Bosworth 2015). The syn-rift group are normal rotational faults resulting from the gravity collapse of the 40-km thick Arabian shield into the Red Sea rift. In most places along the Red Sea coast of Saudi Arabia the two fault systems are parallel and because both systems can dip either to the east or west it is sometimes difficult to distinguish between such structures present in the field as long narrow wadis bounded by high hills or mountains. However, in the Rabigh area the pre-rift faults are truncated by one of the syn-rift faults. This was named the “Master Listric Fault” system by Roobol and Kadi (2008) and it can be traced along the length of the Red Sea where it separates the Precambrian shield from the Cenozoic sediment of the Red Sea coastal plain.

The pre-rift faults are most common in the foothills in Precambrian rocks that border the Red Sea coastal plain and decrease in numbers eastward toward the Red Sea escarpment. Roobol and Kadi (2008) named this fault system the Foothills Fault System. The syn-rift faults are poorly exposed in the gravel and in poorly consolidated Tertiary sediments of the Red Sea coastal plain but have been proved by drilling. Roobol and Kadi (2008) named this group of faults the “Red Sea Coastal Plain Faults”. Roobol and Kadi (2008) regard the Rabigh area as the best locality to distinguish the two fault systems because it is the only place

where the two sets have different orientations. Previously in areas where they are parallel they have not been distinguished and were named the “Red Sea Fault System”.

Previous workers have regarded all these faults as normal rotational faults, but the presence of the major gabbro dikes in them and the accuracy of being able to position them on the published aeromagnetic map of western Saudi Arabia (Zahran et al. 2003) have resulted in a new interpretation for the pre-rift faults. In the Rabigh area, Roobol and Kadi (2008) used 1:50,000 topographic and aeromagnetic images, where it was possible to identify the signatures of hidden dikes that followed the faults and sometimes stepped across from one fault to another. Because the aeromagnetic signatures of the gabbro dikes (which run along the length of the Red Sea, cf. Blank 1977) are sharp and distinct, it can be argued that the pre-rift dikes cannot be curved normal rotational faults near the surface. Instead, the sharp aeromagnetic traces indicate that they must be steeply inclined, at least for the upper several kilometres. The two fault systems are considered to be physically different—the pre-rift faults are steeply inclined planes often hosting major dikes, whereas the syn-rift faults of the Red Sea coastal plain are normal rotational faults (Roobol and Kadi 2008).

Although the numerous northwest-southeast faults in northwest Saudi Arabia (including ribbon faults in the Turayf Group) began forming in pre-rift times (and some may be reactivated pre-Cretaceous faults), geologic and seismic evidence supports the proposition that minor activity continues on them up to the present day. This activity might be regarded as syn-rift reactivation of pre-rift structures. Vaslet et al. (1994) describe the Shagab quadrangle where a tongue of basalt lava that extends northeast from Harrat Uwayrid is down-faulted into a 100 m deep northwest-southeast graben (at $27^{\circ}49'06''\text{N}$, $37^{\circ}21'18''\text{E}$). The uppermost basalt flow is down faulted only 10 m. A K/Ar age for this lava flow yielded 7.1 ± 0.9 Ma. Thus, the graben fault was active after 7.1 Ma. Additional information comes from seismic data from the 1960's onward. Although mainly clustered in the Gulf of Aqaba, there are a number of scattered epicentres well to the east of the Gulf of Aqaba in the area of northwest-southeast Cenozoic faults. In April 2008 an earthquake swarm (maximum magnitude 4.1 at 27.914°N , 37.055°E) occurred in an uninhabited area 75 km southeast of Tabuk and 25 km north of Harrat Uwayrid. This is an area where seismic activity has occurred since instrumental recording began and some epicentres are shown in Figs. 25 and 26. On the surface there are many northwest-southeast Cenozoic faults as well as some oriented both north-south and east-west. The epicentres cannot be correlated with any specific surface fault but correspond to an area of crustal extension with abundant Cenozoic faults.

Comparison of the seismic data layers with the fault map clearly indicates that since instrumental earthquake recording

began, activity in northwest Arabia occurs mainly in the Gulf of Aqaba and represents the Gulf of Aqaba fault system. The seismicity (Figs. 25, 26 and 27) gives little indication of present day activity on either the syn-rift arcuate reactivated Precambrian faults or the prominent east-west fault system. There is some evidence of seismic activity both on the Red Sea coastal plain and just offshore, suggesting some of the syn-rift Red Sea coast plain faults may be still active, or alternatively the seismicity is due to salt tectonics from the Miocene evaporate deposits as seen in the southern coastal city of Jizan, where a salt dome emerges onto the surface.

The seismicity (Figs. 25 and 26) also shows that the ribbon fault system is today mainly inactive. However, some geologic evidence supports syn-rift activity in this system. Many of the horst-graben strips have morphological expressions of a few metres suggesting displacement in the not too distant past. There are also areas of open fissures in some of the Paleozoic sandstone units near Tabuk that indicate crustal extension in the past few thousand years.

The ribbon fault system, as well the pre-rift grabens (some with gabbro dikes), indicate northeast to southwest crustal extension in northwest Saudi Arabia in the form of thousands of small horst and graben blocks. This style of crustal extension in the NW of Saudi Arabia contrasts greatly with the system of crustal extension seen on the west-central part of the Arabian shield, where a well-defined graben system underlies the Cenozoic basaltic lava fields of the Makkah-Madinah-Nafud volcanic line (MMN line). The difference in the physical expression of the crustal extension on the back or passive margin of the Arabian tectonic plate may reflect mainly the physical nature of the host rocks. In the northwest, layered sedimentary rocks of the Phanerozoic cover rocks dominate, whereas in west central Saudi Arabia the Precambrian shield rocks dominate. The different styles of extension may reflect only lithological differences. Such an interpretation is shown in Fig. 28. The extension in the underlying crystalline Precambrian shield is expressed as a simple graben system but in the overlying less competent and unmetamorphosed Phanerozoic cover rocks, the basement faults are shown as feathering or splaying into a fault swarm of many small faults as they penetrate the sedimentary cover rocks.

14 Conclusion

Today the most seismically active area of Saudi Arabia is centred on the Gulf of Aqaba and extends to the shores on both sides. The distribution of the epicentres corresponds to the pattern of the Gulf of Aqaba fault system. Geological work in the area reveals thousands of young Cenozoic faults, mainly Neogene (younger than 23 Ma), that extend over an

area up to 300 km east of the Gulf of Aqaba. In this area to the east of the Gulf there are many fault systems of different ages. Some faults predate rifting of the Red Sea, such as the Tabuk graben that aeromagnetic data shows to be underlain by the Great Ja'adah Gabbro Dike. This dike is actually about 30–40 km to the northeast of a much more subdued magnetic trend that passes close to the city of Tabuk. The Ja'adah dike (or Tabuk graben) extends northwest out of Saudi Arabia up to the Dead Sea Rift Zone (cf. Hatcher et al. 1981), as is also indicated by the fault trends shown in the geological map of Jordan (Bender 1975). Some of the northwest-southeast faults of this system show seismic activity and can be regarded as syn-rift reactivation of older pre-rift faults. The current earthquake record contains little evidence for the thousands of Cenozoic faults in the 300-km wide area east of the Gulf of Aqaba.

At the present time there is considerable development of infrastructure and new towns and cities throughout Saudi Arabia. From Haql and the Saudi Arabian side of the Gulf of Aqaba, the high-rise hotels of Elat and Sharm el Shaik can be seen, and there is the possibility of developing hotels and a tourist industry on the Saudi Arabian side of the Gulf. However, the work of Ben-Avraham et al. (1979) and Ben-Avraham (1985) clearly shows that active faults underlying the Gulf of Aqaba pass close to the Saudi Arabian side of the Gulf. Roobol et al. (1999) describe an area of epicentral rupture of the ground along the Saudi Arabian coastline between Haql and Maqna. The fault map (Fig. 7) shows the distribution of the active Gulf of Aqaba fault system and its proximity to the Saudi Arabian coastline. Hence any future development along the shoreline of the Saudi Arabian side of the Gulf of Aqaba must take into consideration the close proximity of major faults belonging to the Gulf of Aqaba system to the Saudi Arabian shore. The danger of development in a coastal area of potential epicentral rupture, sand volcano formation (due to P wave expulsion of groundwater) and small tsunamis (as was observed to happen in November 1995) must be considered.

Acknowledgements The work was initiated in 2003 by the geohazard section of the Saudi Geological Survey, when raised coral reefs were surveyed along the coast of the Gulf of Aqaba by a team comprising John Roobol, Mohammed Al Rehaili, Ghassan Al-Sulaimani, Faisal Al-Ammawi, and A.A. Al-Gafour Turkostani and was completed by the National Center for Earthquakes and Volcanoes, partly as compilation work and partly as a field traverse accompanied by Mr. Khalid A. Kadi. The earthquake database was edited by Dr. S.Y. El-Hadidy. The data is released with the permission of President of the Saudi Geological Survey, His Excellency Dr. Z.A. Nawab. The SRTM and magnetic data processing and images in the report employ software from Stewart Geophysical Consultants Pty. Ltd. (stewgeop@senet.com.au). Drafting of the diagrams was done by Mr. Diosado G. Quero, Mr. George Certeza and Mr. Mazen Abuabdullah.

References

- Abdel-Rahman K, Al-Amri AMS, Abdel-Moneim E (2009) Seismicity of the Sinai Peninsula, Egypt. *Arabian J Geosci* 2:103–118
- Alabouvette B, Motti E, Redmond CP, Villemur JR (1979) The Wadi Azlam prospect—results of the 1974 program. Saudi Arabian Directorate General of Mineral Resources, BRGM Saudi Arabian Mission Report 97-JED-15, 38 p, 7 figs, 21 app
- Al Amri AM, Schult FR, Bufe CG (1991) Seismicity and aeromagnetic features of the Gulf of Aqaba (Elat) region. *J Geophys Res* 96 (B12):179–185
- Al Tarazi E, Abu Rajab J, Gomez F, Cochran W, Jaafar R, Ferry M (2011) GPS measurements of nearfield deformation along the southern Dead Sea Fault System. *Geophys Geochem Geosyst* (G3) 12(12). <https://doi.org/10.1029/2011gc003736>, 17 p
- ArRajehi A, McClusky S, Reilinger R, Daoud M, Alchalbi A, Ergintav S, Gomez F, Sholan J, Bou-Rabee F, Ogubazghi G, Haileab B, Fisseha S, Asfaw L, Mahmoud S, Rayan A, Bendik R, Kogan L (2010) Geodetic constraints on present-day motion of the Arabian Plate: Implications for Red Sea and Gulf of Aden rifting. *Tectonics* 29, TC3011. <https://doi.org/10.1029/2009tc002482>, 10 p
- Bayer H-J, Hotzl H, Jado AR, Roscher B, Voggenreiter W (1988) Sedimentary and structural evolution of the northwest Arabian Red Sea margin. *Tectonophysics* 153:137–151
- Bazzari M, Merghelani H, Badawi H (1990) Seismicity of the Haql Region, Gulf of Aqaba, Kingdom of Saudi Arabia. Saudi Arabian Directorate General of Mineral Resources Open-File Report USGS-OF-10-9 (IR 825), 39 p
- Bender F (1975) Geologic map of Jordan. Scale 1:500,000. U.S. Geological Survey, Reston, Virginia, Professional paper 560-I, Plate 1
- Ben-Avraham Z (1985) Structural framework of the Gulf of Elat (Aqaba), northern Red Sea. *J Geophys Res* 90(B1):703–716
- Ben-Avraham Z, Garfunkel Z, Almagor G, Hall JH (1979) Continental breakup by a leaky transform: the Gulf of Elat (Aqaba). *Science* 206:214–216
- Ben-Avraham Z, Garfunkel Z, Lazar M (2008) Geology and evolution of the Southern Dead Sea Fault with emphasis on subsurface structure. *Ann Rev Earth Planet Sci* 36:357–387
- Ben-Menahem A, Aboodi E (1981) Micro- and macro seismicity of the Dead Sea Rift and off-coast eastern Mediterranean. *Tectonophysics* 80:199–233
- Blank HR (1977) Aeromagnetic and geological study of Tertiary dikes and related structures on the Arabian margin of the Red Sea. Saudi Arabian Directorate General of Mineral Resources, Red Sea Research 1970-1975, Bulletin no. 22, pp G1-18
- Blank HR, Andresen GE (1991) Compilation and interpretation of aeromagnetic data for the Precambrian Arabian shield, Kingdom of Saudi Arabia. Saudi Arabian Directorate General of Mineral Resources Open-File Report USGS-OF-10-8, 54 p
- Bohannon RG, Nasser CW, Schmidt DL, Zimmermann RA (1989) The timing of uplift, volcanism, and rifting peripheral to the Red Sea: a case for passive rifting? *J Geophys Res* 94:1683–1701
- Bosworth W (2015) Geological evolution of the Red Sea: Historical background, review and synthesis. In: Rasul NMA, Stewart ICF (eds) *The Red Sea: the formation, morphology, oceanography and environment of a young ocean basin*. Springer Earth System Sciences, Berlin Heidelberg, pp 45–78. https://doi.org/10.1007/978-3-662-45201-1_3
- Camp VE, Roobol MJ (1992) Upwelling asthenosphere beneath western Arabia and its regional implications. *J Geophysics Res* 97 (B11):15255–15271
- Clark MD (1987) Geological map of the Al Bad Quadrangle, sheet 28A: Kingdom of Saudi Arabia. Saudi Arabian Directorate General of Mineral Resources Geoscience Map GM-81C, scale 1:250,000, with text, 46 p
- Coleman RG (1977) Geologic background of the Red Sea. In: Red Sea Research (anon. ed.) Saudi Arabian Directorate General of Mineral Resources Bulletin no. 22:C1-C9
- Daëron M, Klinger Y, Tapponier P, Elias A, Jacques E, Surssock A (2007) 12,000-year-long record of 10 to 13 paleoearthquakes on the Yammouneh Fault, Levant Fault System, Lebanon. *Bull Geol Soc Am* 97(3):749–771
- Davies FB, Grainger DJ (1985) Geologic map of the Al Muwaylih quadrangle, sheet 27A, Kingdom of Saudi Arabia. Saudi Arabian Deputy Ministry for Mineral Resources Geoscience Map GM-82A, scale 1:250,000, with text 32 p
- Dogliioni C, Carminati E, Bonatti E (2003) Rift asymmetry and continental uplift. *Tectonics* 22(3):1024. <https://doi.org/10.1029/2002tc001459>
- El-Isa ZH, Merghelani HM, Bazzari MA (1984) The Gulf of Aqaba earthquake swarm of 1983 January–April. *Geophys J Roy Astron Soc* 78:711–722
- Eyal M, Bartov Y, Shimron AE, Bentor YK (1980) Sinai geological map. *Geol Surv Isr*, Scale 1:500,000
- Eyal M, Eyal Y, Bartov Y, Steinitz G (1981) The tectonic development of the western margin of the Gulf of Elat (Aqaba) rift. *Tectonophysics* 80:39–66
- Gettings ME, Blank HR, Mooney WD, Healy JH (1986) Crustal structure of southwestern Saudi Arabia. *J Geophys Res* 91:6491–6512
- Girdler RW, Southren TC (1987) Structure and evolution of the northern Red Sea. *Nature* 330:716–721
- Grainger DJ, Hanif MR (1989) Geologic map of the Shagab quadrangle, sheet 27B, Kingdom of Saudi Arabia. Saudi Arabian Directorate General of Mineral Resources Geoscience Map GM-109C, scale 1:250,000, with text 31 p
- Hamiel Y, Amit R, Begin ZB, Marco S, Katz O, Salamon A, Zilberman E, Porat N (2009) The seismicity along the Dead Sea fault during the last 60,000 years. *Bull Seismol Soc Am* 99:2020–2026
- Hatcher RD, Zietz I, Regan RD, Abu-Ajamieh M (1981) Sinistral strike slip motion on the Dead Sea Rift: Confirmation from new magnetic data. *Geology* 9:458–462
- Hayes TS, Sutley SJ, Kadi KA, Balkhiyour MB, Siddiqui AA, Beshir Z, Hashem HI (2002) Jabal Dhaylan zinc-lead deposits, geological setting, genesis and 1996–2000 exploration progress. Saudi Geological Survey Open-File Report SGS-OF-2001-5; vol.1—Text, App 1 and Plates; vol. 2—Apps 2, 3, 4 and 5; text 71 p
- Hughes GW, Filatoff J (1994) New biostratigraphic constraints on Saudi Arabian Red Sea pre- and syn-rift sequences. In: Al-Husseini MI (ed) *Middle East Petroleum Geosciences Conference, Geo'94*, April 25–27, 1994, Bahrain. Selected Paper, Gulf Petrolink, Manama, Bahrain, vol. II: 517–528
- Hughes GW, Johnson RS (2005) Lithostratigraphy of the Saudi Arabian Red Sea. *GeoArabia* 10(3):49–126
- Janjou D, Halawani MA, Al-Muallem MS, Robelin C, Brosse J-M, Courbouleix S, Dagain J, Genna A, Razin T, Roobol MJ, Shorbaji H, Wyns R (1996) Geologic map of the al-Qalibah quadrangle, sheet 28C, Kingdom of Saudi Arabia. Saudi Arabian Directorate General of Mineral Resources Geoscience Map GM-135, scale 1:250,000, with text 44 p
- Janjou D, Halawani MA, Brosse J-M, Al-Muallem MS, Becq-Giraudon J-S, Dagain J, Genna A, Razin T, Roobol MJ, Shorbaji H, Wyns R (1997) Geologic map of the Tabuk quadrangle, sheet 28B, Kingdom of Saudi Arabia. Saudi Arabian Deputy Ministry for Mineral Resources Geoscience Map GM-137, scale 1:250,000, with text 49 p

- Johnson PR (1998) Tectonic map of Saudi Arabia and adjacent areas. Saudi Arabian Deputy Ministry for Mineral Resources Technical Report USGS-TR-98-3 (IR 948)
- Johnson PR (2007) Geologic map of the Sirhan-Turayf Basin compiled by P.R. Johnson after mapping by Chester A. Wallace, Salah M. Dini, Anwar A. al-Farasani, Ahmed S. Banaker, Abdullah F. al-Khattabi and Mohammed H. al-Kaff. Saudi Geological Survey, unpublished map, scale 1:250,000
- Johnson PR, Vranas GJ (1992) Qualitative interpretation of aeromagnetic data for the Arabian shield. Saudi Arabian Directorate General of Mineral Resources Open-File Report USGS-OF-92-1, 34 p
- Klinger Y, Rivera L, Haessler H, Maurin J-C (1999) Active faulting in the Gulf of Aqaba: New knowledge from the Mw 7.3 earthquake of 22 November 1995. *Bull Seismol Soc Am* 89:1025–1036
- Klinger Y, Michel R, Avouac J-P (2000a) Co-seismic deformation during the Mw 7.3 Aqaba earthquake (1995) from ERS-SAR interferometry. *Geophys Res Lett* 27(22):3651–3654
- Klinger Y, Avouac JP, Dorbath L, Abou Karaki N, Tisnerat N (2000b) Seismic behavior of the Dead Sea fault along Araba valley, Jordan. *Geophys J Int* 142:769–782
- Klinger Y, Le Béon M, Al-Qaryouti M (2015) 5000 yr of paleoseismicity along the southern Dead Sea fault. *Geophys J Int* 202:313–327
- Liddicoat WK (1982) Cenozoic volcanic pipes in the Marythoum area (27/37D). Saudi Arabian Deputy Ministry for Mineral resources, Jeddah, Open-File Report DGMR-OF-03-11, 47 p
- Makris J, Allam A, Mokhtar T, Basahel A, Dehghani GA, Bazari M (1983) Crustal structure in the northwestern region of the Arabian shield and its transition to the Red Sea. *Bull Faculty Earth Sci, King Abdulaziz University*, 6:435–447
- McGuire AV, Bohannon RG (1989) Timing of mantle upwelling: Evidence for a passive origin for the Red Sea rift. *J Geophys Res* 94:1677–1682
- Mitchell NC, Stewart ICF (2018) The modest seismicity of the northern Red Sea rift. *Geophys J Int* 214:1507–1523
- Motti E, Teixido L, Vazquez-Lopez R, Vial A (1982) Maqna Massif area—Geology and Mineralization. Saudi Arabian Deputy Ministry for Mineral Resources Open-File Report BRGM-OF-02-16, 44 p
- Phoenix Corporation (1985) The interpretation of an airborne geophysical survey of the Cover Rocks region. Kingdom of Saudi Arabia, Saudi Arabian Deputy Ministry for Mineral Resources, 76 p
- Reillinger R, McClusky S, Vernant P, Lawrence S, Ergintav S, Cakmak R, Ozener H, Kadirov F, Guliev I, Stepanyan R, Nadariya M, Hahubia G, Mahmoud S, Sakr K, ArRajehi A, Paradissis D, Al-Aydrus A, Prilepin M, Guseva T, Evren E, Dmitrotsa A, Filikov SV, Gomez F, Al-Ghazzi R, Karam G (2006) GPS constraints on continental deformation in the Africa-Arabia-Eurasia continental collision zone and implications for the dynamics of plate interactions. *J Geophys Res* 111, B05411. <https://doi.org/10.1029/2005jb004051>, 26 p
- Reillinger R, McClusky S, ArRajehi A (2015) Geodetic constraints on the geodynamic evolution of the Red Sea. In: Rasul NMA, Stewart ICF (eds) *The Red Sea: The formation, morphology, oceanography and environment of a young ocean basin*. Springer Earth System Sciences, Berlin Heidelberg, pp 135–149. https://doi.org/10.1007/978-3-662-45201-1_7
- Roobol MJ, Al-Rehaili M, Arab N, Celebi M, Halawani MA, Janjou D, Kazi A, Martin C, Sahl M, Showail A (1999) The Gulf of Aqaba Earthquake of 22 November, 1995: Its effects in Saudi Arabia. Saudi Arabian Deputy Ministry for Mineral Resources Technical Report BRGM-TR-99-16, 67 pp, 49 figs, 4 tables, 1 app
- Roobol MJ, Kadi KA (2008) Cenozoic faulting in the Rabigh area, central west Saudi Arabia (including the sites of King Abdullah Economic City and King Abdullah University for Science and Technology). Saudi Geological Survey Technical Report SGS-TR-2008-6, 1:250,000 map, with text 12 p
- Roobol MJ, Stewart ICF (2009) Cenozoic faults and recent seismicity in northwest Saudi Arabia and the Gulf of Aqaba region. Saudi Geological Survey Technical Report SGS-TR-2008-7, 35 pp, 35 figs, 2 apps, 10 plates
- Rowaihi MN (1985) Geological map of the Haql quadrangle, sheet 29A, Kingdom of Saudi Arabia. Saudi Arabian Directorate General of Mineral Resources Geoscience Map GM-80C, scale 1:250,000, with text 15 p
- Sadeh M, Hamiel Y, Ziv A, Bock Y, Fang P, Wdowinski S (2012) Crustal deformation along the Dead Sea Transform and the Carmel Fault inferred from 12 years of GPS measurements. *J Geophys Res* 117, B08410. <https://doi.org/10.1029/2012jb009241>, 14 p
- Sawires R, Peláez JA, Fat-Helbary RE, Ibrahim HA (2016) Updated probabilistic seismic-hazard values for Egypt. *Bull Seismol Soc Am* 106:1788–1801
- Smith J, Bokhari M (1984) The Haql Earthquake; preliminary report for the period 6–30 Rabi al Thani, 1403/ January-February, 1983. Saudi Arabian Directorate General of Mineral Resources Open-File Report DGMR-OF-03-29, 12 p
- Stewart ICF (2007) Earthquake risk in western Saudi Arabia and the Red Sea from seismic moment. Saudi Geological Survey Technical Report SGS-TR-2007-4, 41 pp, 32 figs
- Vaslet D, Janjou D, Robelin C, Al-Muallem MS, Halawani MA, Brosse J-M, Breton J-P, Courboulis S, Roobol MJ, Dagain J (1994) Geologic map of the Tayma Quadrangle, Sheet 27C, Kingdom of Saudi Arabia. Saudi Arabian Directorate General of Mineral Resources Geoscience Map GM-134, scale 1:250,000, with explanatory text 51 p
- Wallace CA, Dini SM, Al-Farasani AA (2000a) Geologic map of the Thaniyat Turayf quadrangle, sheet 29C, Kingdom of Saudi Arabia. Saudi Geological Survey Geoscience Map GM-129C, scale 1:250,000 with text 31 p
- Wallace CA, Dini SM, Al-Farasani AA (2000b) Geologic map of the Wadi as Sirhan quadrangle, sheet 30C, Kingdom of Saudi Arabia. Saudi Geological Survey Geoscience Map GM-127C, scale 1:250,000 with text 27 p
- Wallace CA, Dini SM, Al-Farasani AA (2001) Geologic map of the Jibal at Tubayq quadrangle, sheet 29B, Kingdom of Saudi Arabia. Saudi Geological Survey Geoscience Map GM-133C, scale 1:250,000 with text 36 p
- Wetzler N, Kurzon I (2016) The earthquake activity of Israel: Revisiting 30 years of local and regional seismic records along the Dead Sea Transform. *Seismol Res Lett* 87(1):47–58
- Williams VS, Al-Rehaili MH, Al-Sulaimani G, Showail AA, Bahloul S, Zahrani M (2001) Preliminary report on investigations of neotectonics and paleoseismicity on the east coast of the Gulf of Aqaba. Saudi Geological Survey Open-File Report SGS-OF-2001-2, 11 p
- Zahrani HM, Stewart ICF, Johnson PR, Basahel MH (2003) Aeromagnetic-anomaly maps of central and western Saudi Arabia. Saudi Geological Survey Open-File Report SGS-OF-2002-8, 6 pp, 1 fig, 1 table, 4 sheets (scale 1:2,000,000)
- Zahrani HM, Sokolov V, El-Hadidy Youssef S, Alraddadi WW (2015) Preliminary probabilistic seismic hazard assessment for the Kingdom of Saudi Arabia based on combined areal source model: Monte Carlo approach and sensitivity analyses. *Soil Dynamics Earthquake Eng* 77:453–468
- Zahrani HM, Sokolov V, Roobol MJ, Stewart ICF, El-Hadidy Youssef S, El-Hadidy M (2016) On the development of a seismic source zonation model for seismic hazard assessment in western Saudi Arabia. *J Seismology*. <https://doi.org/10.1007/s10950-016-9555-y>, 23 p